

Review

New Developments and Future Trends in Low-Temperature Hot Stamping Technologies: A Review

Chenpeng Tong ¹, Qi Rong ¹, Victoria A. Yardley ¹, Xuetao Li ², Jiaming Luo ², Guosen Zhu ² and Zhusheng Shi ^{1,*} 

¹ Department of Mechanical Engineering, Imperial College London, London SW7 2AZ, UK; chenpeng.tong17@imperial.ac.uk (C.T.); q.rong15@imperial.ac.uk (Q.R.); v.yardley@imperial.ac.uk (V.A.Y.)

² Shougang Research Institute of Technology, Shougang Group, Beijing 100041, China; lxt@shougang.com.cn (X.L.); jiamingluo@shougang.com.cn (J.L.); zhuguosen@shougang.com.cn (G.Z.)

* Correspondence: zhusheng.shi@imperial.ac.uk; Tel.: +44-20-7594-9546

Received: 13 November 2020; Accepted: 2 December 2020; Published: 8 December 2020



Abstract: Improvement of the hot stamping process is important for reducing processing costs and improving the productivity and tensile properties of final components. One major approach to this has been to conduct all or part of the process at lower temperatures. The present paper reviews the state of the art of hot stamping techniques and their applications, considering the following aspects: (1) conventional hot stamping and its advanced developments; (2) warm stamping approaches in which complete austenitisation is not attained during heating; (3) hot stamping with a lower forming temperature, i.e., low-temperature hot stamping (LTHS); (4) advanced medium-Mn steels with lower austenitisation temperatures and their applicability in LTHS. Prospects for the further development of LTHS technology and the work required to achieve this are discussed.

Keywords: low-temperature hot stamping; hot stamping; warm stamping; low heating temperature; low forming temperature; medium-Mn steel; cost-saving; productivity; mechanical property

1. Introduction

Owing to the depletion of non-renewable energy resources and the environmental impact of burning fossil fuels, there has been a strong push to improve the fuel efficiency of automobiles in recent years. One of the most feasible approaches is by light-weighting; a 10% weight reduction can lead to an almost 2.5% increase in fuel efficiency [1]. The automotive industry is thus working on reducing vehicle weights with simultaneous improvements in safety and crashworthiness. This can often be achieved either by using lighter materials, such as aluminium alloys, or by using stronger materials such as advanced high strength steels (AHSS) in the body in white (BiW) of vehicles. Hot stamping technology has been developed as a specialised production technique for the manufacture of components from AHSS; this addresses the shortcomings encountered in conventional cold forming technologies, such as poor formability, high impact on the tools and an elevated tendency to springback [2]. The most commonly used AHSS materials are boron (Mn-B) steels, such as 20MnB5, 22MnB5 and 27MnCrB5, which show a yield strength (YS) of above 770 MPa and an ultimate tensile strength (UTS) of above 1300 MPa with a total elongation (TE) of around 6–8% in hot-stamped parts [3]. The most notable example to date of the application of hot-stamped AHSS in the automotive sector is the 2014 Volvo XC90, where hot-stamped sheet steel was applied for around 38% of the BiW, including the front- and rear-side longitudinal members, A-, B- and C-pillar reinforcements, roof rail reinforcements and floor cross members [4]. The 2014 Acura MDX was another notable example, in which hot-stamped steel was adopted for the A- and B-pillars, roof rail and sill reinforcements [5].

Hot stamping technology for Mn-B steels is now mature and has been commercialised internationally, especially for sheet in the 1500 MPa UTS class. The process chain is illustrated in Figure 1a [6] and a schematic representation of the thermomechanical cycle and the microstructural evolution during the hot stamping process is shown in Figure 1b [7]. During the process, the steel coil is first cut into blanks, heated up to 900–950 °C in a furnace and held isothermally for around 5–10 min until the initial ferrite-pearlite microstructure is completely transformed to austenite [7]. The blanks are subsequently transferred from the furnace to a press, where they are formed at around 700 °C or higher, then quenched to room temperature with a cooling rate of at least 27 °C s⁻¹, this being the critical rate necessary to obtain a fully martensitic transformation in the material, assuring ultimate tensile strength of up to 1700 MPa [8]. Finally, the hot-stamped part is post-treated, applying processes such as tempering, trimming and punching, to satisfy the requirements of commercial customers [1]. Much research into hot stamping technology has already been published. For instance, Karbasian [3] has summarised the hot stamping procedure including the thermal, mechanical, microstructural, and technological aspects and has shown the potential for further investigations. Merklein and Lechler [9] have reported that hot-stamped 22MnB5 steel parts could be produced with an ultimate tensile strength of 1500 MPa. Naderi et al. [10] have investigated and analysed the microstructural evolution and corresponding mechanical properties in B-pillars with different designs during the hot stamping process.

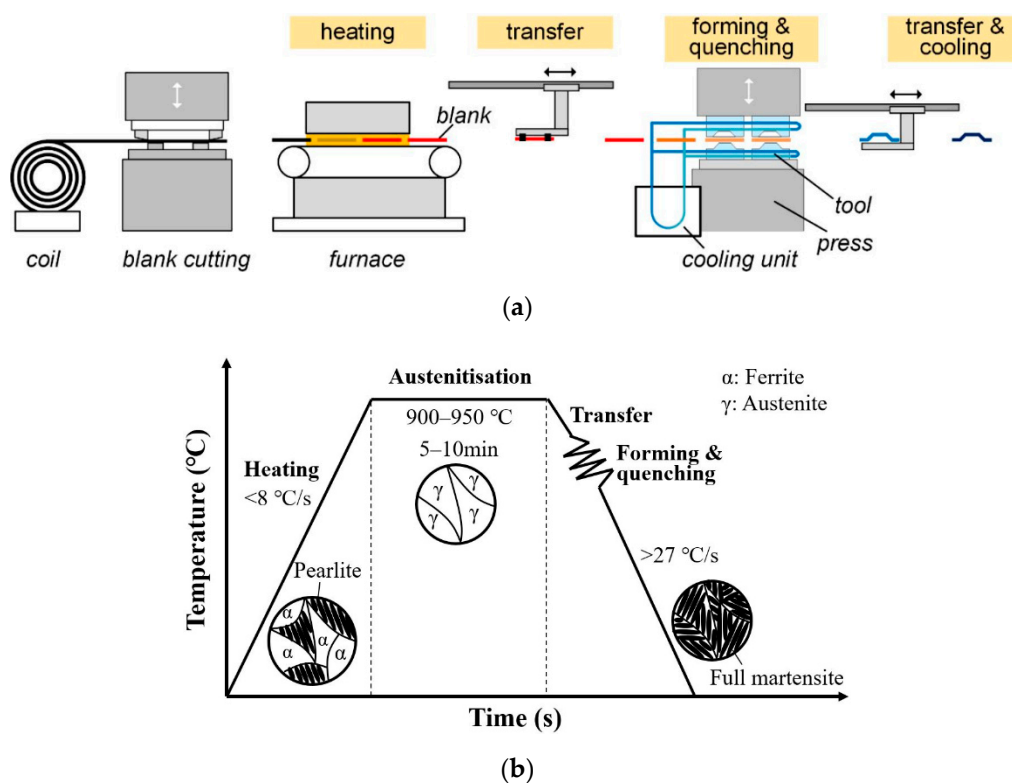


Figure 1. Illustration of conventional hot stamping process for Mn-B steel: (a) Basic hot stamping process chain [6] (Reproduced with permission of Pentera, 2020). (b) Thermomechanical cycle and microstructural evolution during hot stamping.

However, the current hot stamping technology has the following inadequacies [11,12]: (1) The productivity is low due to a long cycle time including both heating and cooling. (2) The cost of protection against oxidation and decarburisation, such as coating or fabrication in an oxygen-free environment, is high. (3) Due to a low ductility, the product is unsuitable for use in energy-absorbing structures. (4) The process requires a large investment in production equipment (including a cooling system with complex design, large furnace and laser trimming).

Due to the globally increasing demand for application of the hot stamping technology within automobile manufacture, there has been great interest in solving these issues. In recent years, several technologies have been developed to improve the production efficiency and enhance the final performance of hot-stamped components. Section 2 of this paper briefly introduces these recent developments in hot stamping. However, the improvements achieved are still not sufficient and these technologies have not been widely implemented in industrial production. Another approach that has recently attracted a great deal of research attention is that of conducting the process at lower temperatures than are typical in the current conventional hot stamping process. This can significantly reduce the process cycle time and save energy and cost. These desired objectives can be achieved through reducing the heating temperature and/or forming temperature and using advanced materials with lower austenitic transformation temperatures (A_1 and A_3), e.g., medium-Mn steel (MMn) steels [13–15]. Recent developments in hot stamping technology with reduced temperatures are critically reviewed in Section 3, including both warm stamping and low-temperature hot stamping (LTHS). Section 4 covers the mechanical behaviour and microstructural mechanisms of MMn steels which good candidates for LTHS. The application of MMn steels in LTHS processes is reviewed in Section 5. Section 6 summarises the conclusions and prospects for future developments in this field.

2. Recent Developments in Hot Stamping

Many novel techniques have been proposed and developed to improve the hot stamping process from the points of view of cost savings, productivity and final performance of hot-stamped components. These technologies include advanced approaches to heating, stamping, die-quenching and post-form treatment, as well as the use of tailored heating and quenching and partitioning (Q&P) techniques [16–19].

2.1. Advanced Approaches to Heating

Alternative heating technologies, such as electrical resistance heating, induction heating, and direct contact heating (illustrated schematically in Figure 2), as well as infrared heating, have been used to improve the productivity and energy efficiency by shortening the heating time with respect to that achievable using the conventional roller hearth furnace [17,18]. These alternative techniques can also reduce the size of the equipment required. Mori et al. [20] proposed the use of rapid electrical resistance heating in hot stamping (Figure 2a). They suggested that the blanks could be heated up to 800–900 °C in only 2 s by connecting two pairs of electrodes; this approach almost eliminates the formation of oxide scale that occurs during longer heating times. Zhang et al. [21] have demonstrated experimentally the feasibility and merits of resistance heating in B1500HS boron steel. However, resistance heating cannot create a uniform distribution of temperature in the blank during the hot stamping process, and this results in poor formability and final mechanical properties. Kollek et al. [22] proposed an advanced rapid heating method using induction heating (Figure 2b), which was implemented through an induction coil carrying high-frequency alternating current (AC). A related method, which used elliptical induction coils to uniformly and rapidly heat 1.2-mm-thick boron steel, was successfully invented, investigated and shown to give good final quality by Kim et al. [23]. Vibrans et al. [24] integrated an induction heating device into a conventional heating line to heat up the sheet rapidly to around 950 °C, after which it was transferred for soaking to a roller hearth furnace. This novel design gave a time saving of about 50% with respect to the conventional process, while avoiding the problem of non-uniform heating. Recently, Ploshikhin et al. [25,26] have proposed the application of a direct contact heating method (Figure 2c) in which the sheets are press-heated by two hot plates. A heating cycle time of only around 30 s is required to fully austenitise a typical Al-Si-coated boron steel and a good uniform temperature distribution is achieved. This technique requires less production space and has a higher energy efficiency than heating using a roller hearth furnace. In addition, infrared radiation has also been considered as a novel heating method, but this has a relatively low heating rate compared to the methods introduced above. It can be classified into far and near types [20]. Far-infrared heating

is good for temperature control and has been gradually developed to be employed in the hot stamping industry [27,28]. Near-infrared heating has a higher conversion efficiency but with poor temperature control capabilities. Hence, investigations have so far focused on partial heating or local heating. Lee et al. [29,30] used near-infrared heating devices to locally heat non-quenchable AHSS to reduce the springback induced by cold forming. However, most of the processes described above are still limited to laboratory scale and further work is required to determine their viability for industrial applications.

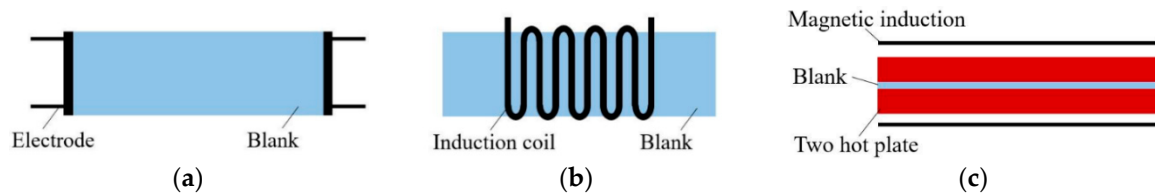


Figure 2. Advanced heating systems for hot stamping: (a) Resistance heating; (b) Induction heating; (c) Direct contact heating.

2.2. Advanced Stamping and Die Quenching Technologies

Optimisation of stamping and die quenching systems is another important way of improving the productivity and the final performance of the hot-stamped parts. As shown in Figure 3, three aspects have been considered and investigated: (1) increasing the contact pressure, (2) increasing the heat transfer area and (3) improving the die and cooling system. Schuler [31] has proposed and developed a new type of hot stamping press tool (Figure 3a), named pressure-controlled hardening (PCH), which uses a hydraulic bed cushion to increase the pressure and thus the contact surface between blank and die. The heat transfer coefficient is increased, resulting in a shorter stamping time and leading to higher productivity. Vollmer et al. [32] and Palm et al. [33] experimentally studied the effectiveness of the PCH cushion, demonstrating an increase in productivity from 2–3 strokes per min (spm) with conventional hot stamping equipment to almost 7–8 spm with the cushion. Figure 3b illustrates an attempt to increase the contact area of heat transfer for blanks by direct injection of water into the inevitable gap between the blank and the die during stamping to avoid poor heat transfer. Maeno et al. [34] conducted a series of tests using this water and die quenching technique. Their results showed not only an improvement of productivity to 10 spm, but also an enhanced formability thanks to the more uniform heat transfer. Although these two methods have begun to be applied in commercial production, they require an increased investment in equipment and the return-on-investment for these techniques has not yet been evaluated.

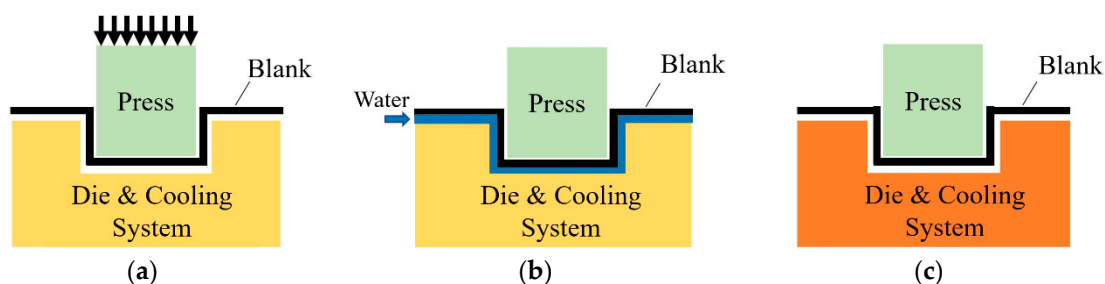


Figure 3. Advanced forming and quenching methods in hot stamping: (a) Increase contact pressure; (b) Improve quenching quality; (c) Improve die and cooling system.

Figure 3c represents other advanced methods adopted in the die and quenching system to improve the heat transfer and the heat and abrasion resistance [35]. Many researchers [36–39] have already made great efforts to develop the cooling channel design by analysing the phase transformations in the blank, the design of die structures and the influence of flow velocity. They have also worked to optimise cooling system parameters, such as the gap between the channels and the depth from the

channels to the die surface, in order to improve the cooling performance and minimise the quenching time. Despite these achievements, the range of applications of such cooling systems is inevitably restricted by their complex design and the high costs of manufacturing and maintenance. In a different approach, Li et al. [40] recently experimentally and numerically investigated the influence of thermal conductivity of dies on the cooling behaviour and final product performance, using five dies with different thermal conductivities. Their results showed that the cooling performance and formability were significantly improved by increasing the thermal conductivity of the die, showing the feasibility of this approach. However, the investment involved in introducing these dies may be too high for commercial application.

2.3. Tailored Microstructures and the Quenching and Partitioning Process

Additionally, in order to improve the final performance of hot-stamped components and widen their application, two novel techniques have been developed, one in which hot stamping is combined with a tailored microstructure [11] and the other in which it is combined with a quenching and partitioning (Q&P) process [41–44]. A typical example of a B-pillar with a tailored microstructure after hot stamping is shown in Figure 4a. Here, the upper region has a higher tensile strength with a fully martensitic microstructure to support the vehicle structure. The lower region has a higher ductility with only a partially martensitic microstructure, the remainder consisting of ferrite and pearlite, to absorb more energy during a possible car crash [11]. Several methods are available to obtain tailored microstructures, such as partial heating, differential cooling, tailor-welded and rolled blanks and partial annealing after hot stamping. [45–52]. For example, Oldenburg [45] used a material combination approach to develop dies comprising materials of different thermal conductivities to achieve different cooling rates as a function of location during the forming stage. This enabled the boron steel microstructure after hot stamping to be tailored. Yun et al. [50] further developed the material combination approach, using lithium nitrate undergoing a phase transformation as the part with low thermal conductivity. This effectively avoided the problem of heat conduction between different materials, and high-quality tailored blanks could be obtained. However, the processes involved in all these approaches are rather complicated and involve extra cost, and the feasibility has so far only been demonstrated on a laboratory scale.

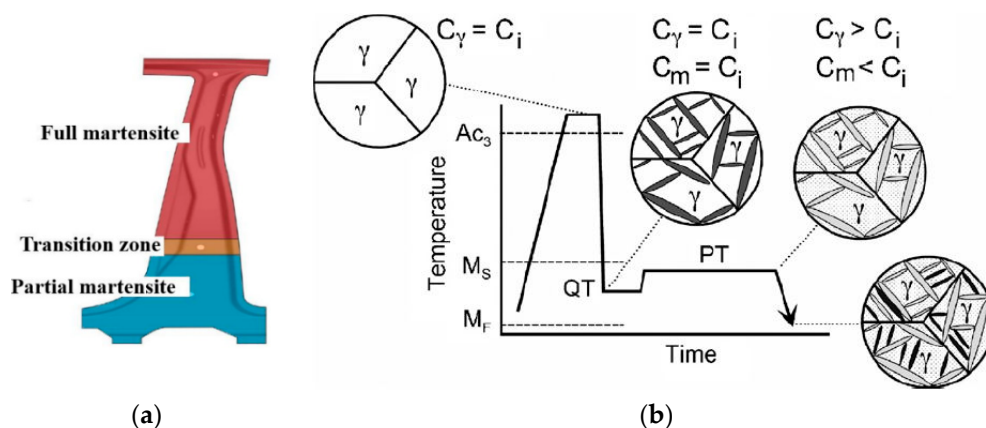


Figure 4. Advanced forming and quenching methods in hot stamping: two novel hot stamping processes for improving the final performance of hot-stamped parts: (a) Tailored microstructure (Adapted with permission from Elsevier [11]); (b) Quenching and partitioning process (reproduced with permission from Elsevier [42]) (C_i , C_γ , C_m represent the carbon contents of the initial alloy, austenite and martensite, respectively).

The Q&P heat treatment process was first proposed by Speer et al. [41–44]. As shown in Figure 4b [42], the treatment starts with a full or partial austenitisation followed by rapid cooling to a quenching temperature (QT) between the martensite start temperature (M_s) and martensite finish

temperature (M_f) to obtain a predesignated fraction of martensite. In the subsequent partitioning treatment, the material is held at a partitioning temperature (PT), which can be equal to QT (one-step treatment) or somewhat higher than QT (two-step treatment) [53,54]. The aim of this novel process is to partition carbon into the austenite and increase the stability of this phase at room temperature, thereby improving the final ductility and toughness through the transformation induced plasticity (TRIP) effect in the retained austenite. Based on this, Liu et al. [55,56] integrated a Q&P treatment into a hot stamping process and examined its efficacy in improving the final performance of conventional hot-stamping boron steel. The ductility was increased from 6.6% to 14.8% after a Q&P treatment at 320 °C for 30 s. Zhu et al. [57] further developed a new hot air system for partitioning; this replaced the conventional furnace to easily and rapidly control the temperature of the blank after quenching with a uniform temperature distribution. However, it is still difficult to achieve isothermal partitioning process in an industrial environment. For the industrial application of Q&P in hot stamping, it is necessary to further investigate the possibility of non-isothermal partitioning and the effect of the Q&P treatment on the impact properties and resistance to hydrogen embrittlement of the steel rather than its ductility only.

2.4. Post-Form Treatments

Finally, post-form treatment processes have also been investigated. Owing to the high strength and hardness of hot-stamped boron steels, wear, chipping and failure in the tools used for post-form machining can cause serious damage, which in turn can lead to high costs and poor productivity [58]. Laser cutting technology is an alternative to mechanical shearing, but it requires high energy input and has a low productivity. Researchers have tried to find different ways to address these shortcomings. For example, Choi et al. [16] have proposed a new hot stamping process for softening local areas and reducing the trimming load, which can improve tool wear. Mori et al. [59] suggested a punching process for AHSS to relax the flow stress in areas with high deformation. So et al. [60] have developed warm blanking as an alternative blanking strategy; here, the temperature of the hot-stamped parts remains above the martensitic transformation temperatures (M_s or M_f) to increase the tool life by reducing the shearing load. In all these methods, it is necessary to improve the structure of the tooling, which could lead to significant additional expense in tool design and manufacturing.

Although, as has been seen, many new developments have been investigated in hot stamping technology in recent years, most of these remain at the level of the laboratory and cannot be applied to benefit industrial production. Recently, however, approaches in which the processing temperature is reduced have attracted much attention owing to their potential as a replacement for conventional hot stamping processes, allowing cost savings, improvements in productivity and better final mechanical properties of stamped parts.

3. Progress in Development of Stamping Processes at Lower Temperatures

One of the main developments proposed to give higher drawability and ductility, reduced occurrence of oxidation (avoiding the need for a protective coating), improved productivity and reduced cost compared to conventional hot forming processes is moving to lower processing temperatures. Two approaches have been considered: (1) conducting the pre-forming heating step and the forming step at a lower temperature than in conventional hot stamping, without achieving full austenitisation and (2) forming at a lower temperature after heating at the same temperature as for conventional hot stamping [13,15,61]. The process for approach (1) is referred to as warm stamping, which will be discussed in detail in Section 3.1. The terminology “hot stamping” is reserved for cases where there is a complete transformation to austenite during the heating step, enabling the production of a fully martensitic microstructure on sufficiently rapid cooling after forming. In this paper, we define “low-temperature hot stamping” (LTHS) as such a hot stamping process carried out at lower temperatures than is the case in conventional hot stamping of boron steels, as in approach (2) above, which is presented in Section 3.2.

3.1. Warm Stamping

Figure 5 shows a schematic of a warm stamping process: the blank is heat-treated under similar conditions to those of the traditional hot stamping process, except that the heating temperature is lower than A_3 (the minimum temperature at which the steel is fully austenitic under equilibrium conditions). The material does not undergo a complete transformation to austenite during the high-temperature parts of the process, and this leads to a microstructure consisting of martensite, ferrite, retained austenite and pearlite at the end of forming, resulting in a lower strength and higher ductility than if full austenitisation were achieved. Research on warm stamping processes has mainly focused on (1) application to conventional AHSS (designed for cold stamping) to reduce the springback and improve the formability and final performance; higher temperatures cannot be used in these cases because this would cause a loss of strength [15,61,62], and (2) boron steels with partial heating to obtain tailored properties and widen their applications [63–65].

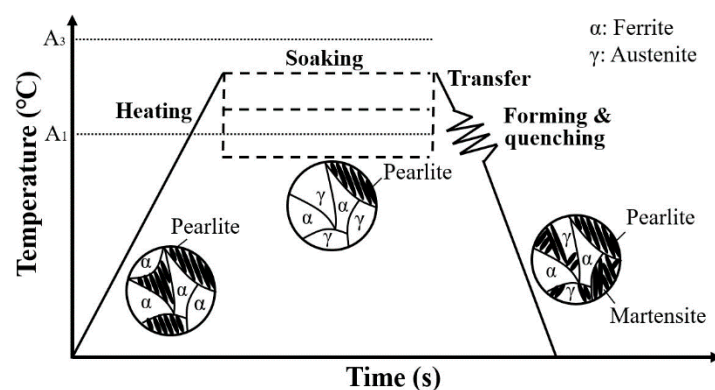


Figure 5. Schematic illustration of hot stamping process with lower heating temperature for Mn-B steel and evolution of microstructure at each stage.

A great advantage of moving to lower temperatures for the heating step is that existing production lines for hot stamping can still be used with a decrease in the heating temperature of the furnace, avoiding heavy capital investment often associated with a new process. Using basic energy equations and furnace parameters, it can be estimated that a reduction of 100 °C in the temperature of the roller hearth furnace is equivalent to a decrease in power of 200 KW/h [66,67]. Thus, a saving of almost 0.2 million GBP of electric power per year could be envisaged by applying this temperature reduction to a single production line for any hot-stamped boron steel part. By controlling the process conditions, it is possible to obtain values of yield strength between 400 and 700 MPa, ultimate tensile strengths between 650 and 1200 MPa and total elongations between 10% and 25%; this is a wider range of strength properties and a higher ductility than is available with conventional hot stamping [61,62].

Mori et al. [61] have experimentally investigated the effect of warm and conventional hot stamping on the springback and formability of ultra-high tensile strength steel sheet (commonly used for cold forming). They suggested that the optimum heating temperature was around 600 °C; this gave minimal springback and oxidation layer thickness combined with the still considerable ultimate tensile strength of 980 MPa. Based on this result, Naderi et al. [15] investigated the feasibility of warm stamping of the steel grade MSW1200 (0.14C–1.71Mn–0.55Cr) developed for cold forming which had an initial yield strength, ultimate tensile strength and total elongation of about 400 MPa, 640 MPa and 26%, respectively. The mechanical properties after conventional cold forming followed by quench hardening (950 °C, 10 min), hot stamping (950 °C, 10 min) and warm stamping (650 °C, 10 min) are listed in Table 1. It can be seen that warm stamping gives lower yield and ultimate tensile strengths than conventional cold forming and hot stamping, but a much higher total elongation. The performance of AHSS is often estimated using the product of ultimate tensile strength and total elongation (UTS × TE) [68]. The results in Table 1 show that a much higher value of this product is obtained in this steel by warm

stamping than using the other processes. The combination of tensile strength and ductility obtained by warm stamping is suitable for application in some automobile parts where high toughness, defined as a good combination of strength and ductility, is required, such as front- and rear-side members.

Table 1. Mechanical properties of MSW 1200 steel after different processes [15].

Type of Steel	YS (MPa)	UTS (MPa)	TE (%)	UTS × TE (GPa·%)
Cold forming + quench hardening	1110	1430	4	5.72
Warm stamping	400	930	20	18.6
Hot stamping	916	1300	5.5	7.15

YS: yield strength; UTS: ultimate tensile strength; TE: total elongation; UTS × TE: the product of UTS and TE.

Recently, many investigations have focused on warm stamping with a rapid heating rate for conventional cold-forming AHSS to further reduce the cycle time and degree of surface oxidation. Mori et al. [62] examined the application of this type of process to ultra-high-strength steel sheet. They found that, while the parts produced showed hardly any improvement in springback after warm stamping, the tensile strength of 1200 MPa and total elongation of 22% achieved allowed these parts to replace some parts produced by conventional hot stamping. This enables much cheaper and easier production while still giving sufficient final performance. In order to further improve the production rate, Sun et al. [69] investigated the effectiveness of a fast warm stamping technique in MS1180 steel sheet, where the temperature for soaking ranged from 300 to 500 °C. The components were stamped immediately after soaking. Good performance of the stamped components, with a post-form tensile strength of 1140 MPa, was achieved for specimens stamped at temperatures of 400–450 °C with a heating rate of over 50 °C s⁻¹; the overall cycle time was less than 10 s. Although ultra-high strength steels exhibit a good combination of strength and ductility after warm stamping, the resulting strengths are insufficient to meet the requirements for car body structures, i.e., >1200 MPa UTS; in addition, it is not possible to reduce the car weight by reducing the thickness of the vehicle parts while retaining the required strength.

Several studies have been carried out with the aim of employing hot stamping boron steel with tailored properties; one of the approaches used was to reduce the heating temperature. Mu et al. [65] examined the effect of heating parameters on the mechanical properties of 22MnB5 steel. They found that the UTS gradually increased from 543 to 1596 MPa with increasing heating temperature in the range 700 to 900 °C due to the increasing extent of austenitisation; the total elongation displayed an opposite trend. Li et al. [63] found a similar result by heating hot stamping boron steels in the temperature range 720–900 °C. However, changes in UTS and TE were insignificant once the heating temperature exceeded 820 °C; this proved to be the threshold required to obtain a certain martensite fraction after quenching. The mechanical properties remained essentially unchanged once this threshold martensite fraction had been reached. Methods of tailoring properties in boron steel using lower heating temperatures are still immature, due to difficulties in controlling temperature gradients. Results so far have shown great potential for the use of reduced heating temperatures in the conventional hot stamping process for boron steel, but further research may be necessary to investigate the minimum heating requirement for acceptable material performance.

3.2. Low-Temperature Hot Stamping

Further improvement in mechanical properties of hot-stamped materials has been attempted by reducing the forming temperature only; in this case, the process is called low-temperature hot stamping. In conventional hot stamping, a completely austenitised blank initially at around 950 °C normally takes about 10–20 s to be quenched to 150–250 °C within a die and cooling system [34]; this is an obstacle to increasing the productivity. Beside this, the die temperature gradually increases during the production of parts quenched from high temperature, leading to severe wear that reduces the lifetime

of the dies [70,71]. To overcome this limitation, as shown in Figure 6, Balint et al. [72] and Ota et al. [73] have proposed a novel process whereby the austenitised steel blanks are pre-cooled to a temperature just above the martensite start temperature before stamping. At this lower forming temperature, strain hardening can be enhanced, improving the drawability and formability; the productivity can also be increased by shortening the cooling cycle time.

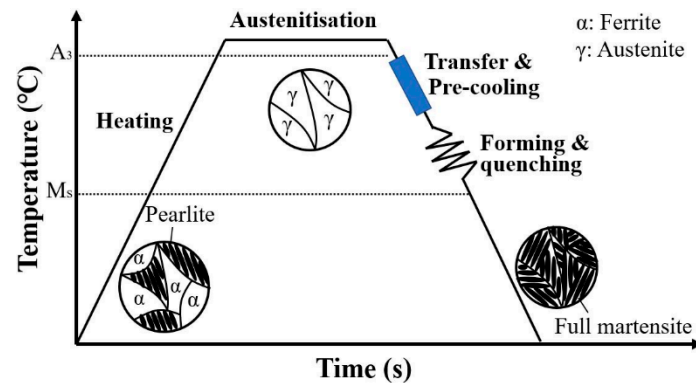


Figure 6. Schematic illustration of hot stamping process for Mn-B steel with lower forming temperature, showing microstructural evolution at each stage.

There are many examples in which the application of this method has been investigated with the aim of improving the performance of hot-stamped components. Tata Steel examined a pre-cooling method in hot stamping to solve the issue of micro-cracking due to high temperature in zinc-coated boron steel, where the coating had been applied to protect against the formation of thick oxide layers [74]. Cracking can theoretically be avoided if the zinc-coated boron steel is hot-stamped at a lower temperature, i.e., between 500 and 740 °C. Nippon Steel and Sumitomo Metal [75], Kobe Steel [76] and ThyssenKrupp [77] have all focused on hot stamping with lower forming temperatures to improve the final performance of parts. Ganapathy et al. [13,78] experimentally investigated an uncoated 22MnB5 steel subjected to this new LTHS process and compared the mechanical properties and productivity to those of the same material subjected to conventional hot stamping. The experimental apparatus used a pre-cooling system of compressed air at 10 bar, giving a fast cooling rate of $>60\text{ °C s}^{-1}$. The temperature was monitored and controlled using calibrated non-contact digital infrared thermometers. The material was heated up and held at 900 °C for about 60 s to give full austenitisation, then pre-cooled to a forming temperature above M_s (around 400 °C for 22MnB5 steel) to guarantee a fully martensitic transformation in the blanks on subsequent quenching. After pre-cooling, the blanks were stamped within the die. The results showed that both the yield strength and ultimate tensile strength had similar values to those seen in conventionally hot-stamped boron steel, with around 1000 MPa YS and 1500 MPa UTS. In addition, the low-temperature hot stamped 22MnB5 steels displayed a more uniform distribution of temperature and a better formability as well as a great improvement in productivity, with a reduction of at least 60% in the required quenching time.

Recently, Ganapathy et al. [79] have proposed another new LTHS process in as-quenched martensitic 22MnB5 steel with the aim of reducing the forming cycle time. As schematically illustrated in Figure 7a, material with an initial microstructure consisting of pearlite and ferrite was heated to 900 °C to be austenitised, followed by rapid quenching to achieve a fully martensitic transformation. Then, the as-quenched material was re-heated to a tempering temperature in the range of 420–620 °C under two alternative heat treatments, (i) fast heating, defined by a total heating time of 50 s and (ii) slow heating, with a total heating time of 100 s. After this, the material was immediately deformed at the tempering temperature, followed by rapid cooling to room temperature. The LTHS conditions were simulated using tensile tests carried out on the as-quenched material using a Gleeble. The strain rate of 1 s^{-1} used in the tests is considered to be representative of the strain rate in industrial production. The peak stress of around 900 MPa obtained by deforming at 420 °C is significantly reduced to around

300 MPa at a deformation temperature of 620 °C, which is good for hot forming. However, in all these experiments significant strain softening was observed. This results in an early onset of necking during deformation, which affects the drawability. In order to investigate the effect of heating conditions on the final performance, the as-quenched boron steels were heated to different tempering temperatures under either the fast or slow heating conditions, then cooled quickly to room temperature (i.e., no hot deformation was carried out). Their room-temperature mechanical properties are shown in Figure 7b. These results show that the room-temperature strength and ductility are decreased with respect to the as-quenched case by heating to the tempering temperature. Both increasing temperature and increasing time (reducing heating rate) lead to further decrease in strength. Thus, the industrial application of this method is not considered to be feasible and the technique requires further improvement.

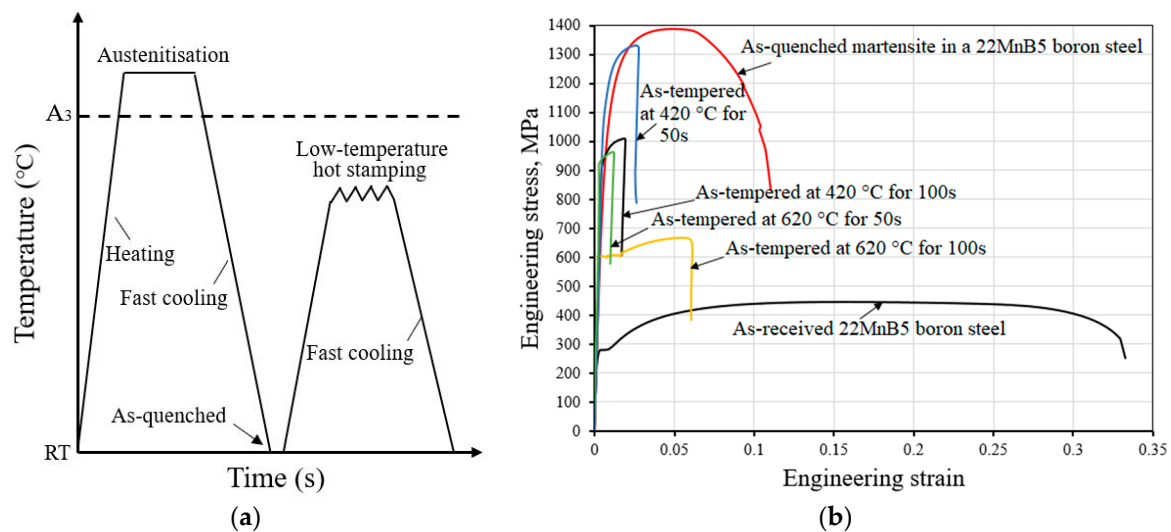


Figure 7. A novel process of low-temperature hot stamping of as-quenched 22MnB5 steel: (a) Schematic representation of the process; (b) room-temperature properties after indicated heat-treatment conditions [79].

These alternative processing methods can give impressive improvements in productivity and formability, but are not able to fully satisfy the expectations of the automotive industry. For instance, with a reduced heating temperature, it is not possible to achieve high strength with thinner components; while with a reduced forming temperature only, thick oxidation and decarburisation layers cannot be avoided and the ductility is still not high enough to widen application in the automotive industry. Therefore, in recent years, attention has been focused on improving the steel grades to overcome these issues [80].

4. New Advanced Materials

4.1. Advanced High-Strength Steels for Automotive Applications

For a long time, steel has been the main material for automobile body structures. Recently, within the development trend of diversification and lightweighting of materials, the total proportion of steel applied in the body-in-white has decreased, but the proportion of advanced high-strength steels (AHSS, YS > 550 MPa) and ultra-high strength steels (AHSS with UTS > 780 MPa) has increased [81,82]. Based on the requirements for light-weighting and crash safety, steels applied in car body structures should have two characteristics: ultra-high strength and high toughness [83]. Figure 8 is a plot of elongation against strength for different families of steels including high strength steel (HSS), and first, second and third generations of AHSS [84]. The most commonly used steels at present for areas of the car body requiring high energy absorption (high toughness) in the event of collision are dual phase (DP) and TRIP steel grades with ultimate tensile strength <1000 MPa [85]. Second-generation advanced high strength steels have the potential

to replace these, but their use is limited due to their high cost. The steels with ultimate tensile strength >1200 MPa are mainly applied for structural elements of the vehicle body to provide a high stiffness and anti-intrusion barrier for the protection of passengers; typical examples are martensitic (MART) and conventionally hot-stamped steels. AHSS sheets used for automotive applications are commonly cold formed, especially those with high toughness, but recently, it has been shown that these materials can be manufactured by warm stamping or even hot stamping to reduce the springback and improve the formability [61,62]. Hot stamping is commonly used for AHSS with good hardenability, such as boron steels, to obtain ultra-high strength with complex shapes. In Figure 8, the combination of mechanical properties obtained by conventional hot stamping of boron steels appears at the bottom right corner; the ultimate tensile strength of such stamped parts is higher than that of most other AHSS, but their ductility is insufficient. The performance of parts formed by the application of warm stamping coincides with the upper-middle level of first-generation AHSS, while the low-temperature hot-stamped parts have a similar performance to parts made using conventional hot stamping.

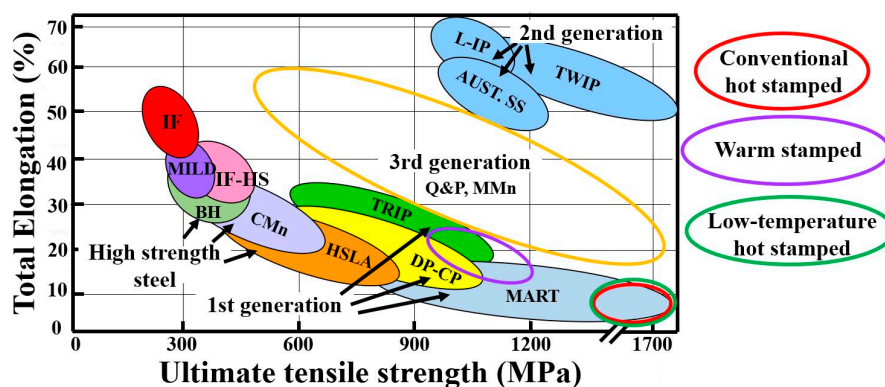


Figure 8. Comparison between mechanical properties of various types of industrially manufactured steel grades and of parts produced by various hot stamping processes. IF: interstitial-free steels; MILD: mild steels; IF-HS: interstitial-free high-strength steels; BH: bake hardening steels; CMn: carbon-manganese steels; HSLA: high-strength low-alloy steels; TRIP: transformation induced plasticity steels; DP-CP: dual phase and complex phase steels; MART: martensitic steels; Q&P: quenching and partitioning steels; MMn: medium-Mn steels; AUST. SS: austenitic stainless steel; L-IP: lightweight steels with induced plasticity; TWIP: twinning-induced plasticity steels.

Third-generation AHSS have been developed not only to meet the stringent requirements of the automotive industry, i.e., excellent mechanical properties (both strength and ductility) at reduced thickness while maintaining high safety standards, but also to avoid the high cost of adding large amounts of alloying elements and the associated processing problems such as poor weldability of second-generation steels [86]. Q&P steels and MMn steels are the main candidates, both of which offer ultra-high strength and high toughness for a relatively low cost. The two types of material have in common that they both use the TRIP or TWIP (twinning-induced plasticity) effect in retained austenite (RA) to increase strength and ductility, the difference being in the method of obtaining the RA. The Q&P process is a novel heat-treatment method for martensitic steels, in which carbon is made to re-partition into the retained austenite remaining after incomplete quenching to martensite. This enhances the stability of the austenite at room temperature. RA fractions of more than 20% can be acquired in Q&P steels, leading to a tensile strength of over 1500 MPa and a value of the product $UTS \times TE$ of more than 30 GPa·% [87,88]. The microstructure in MMn steels is, in contrast, obtained via the austenite reverse transformation (ART) annealing treatment. The quenched and rolled microstructures are heated into the intercritical annealing region (A_1 – A_3) and soaked to acquire ferrite and retained austenite with an ultra-fine grain size [89]. RA fractions of more than 30% can be obtained in MMn steel with ultimate tensile strengths in the range 600–1700 MPa and a product $UTS \times TE$ of more than 30 GPa·% [90].

As a result of this high toughness, both of these types of steels are mainly used for cold forming. Much research effort has been devoted in recent years to improving the final mechanical properties and understanding the deformation mechanisms associated with the enhanced strengthening behaviour in these steels [91–93]. One feature of MMn steels that has attracted particular attention is that the austenitic transformation temperatures (A_1 and A_3) are considerably lower, by around 100–200 °C, than those of conventional hot-stamping boron (Mn-B) steels because of the alloying additions, most importantly Mn. The methods discussed in Sections 3.1 and 3.2, of lowering the heating temperature and the forming temperature in hot stamping, can easily be applied in MMn steels and the benefits of these two processing techniques and of the MMn steel microstructure can be achieved simultaneously. Therefore, MMn steels, a third-generation AHSS type, not only have great prospects for application in cold forming, but also the potential for application in LTHS.

4.2. Medium-Mn Steel

4.2.1. Chemical Composition

Steels of the medium-Mn class can be defined by the composition range of 3–12 wt. % Mn. The other main alloying elements are C, Al and Si; these steels also contain small amounts of other elements such as Mo and V to give further improvements to mechanical properties [14]. The effect of the different alloying elements is summarised below:

1. Carbon is present in all steels. It has a very low solid solubility in ferrite, but a much higher solubility in austenite. In hypoeutectoid steels (<0.77 wt. % C) on sufficiently slow cooling, it is mostly present in the form of lamellae of cementite (Fe_3C) in pearlite. On more rapid cooling, carbon is trapped in solid solution in martensite; subsequent tempering causes the carbon to be precipitated out in the form of cementite which, if carbide-forming elements are present, subsequently dissolves in favour of more stable alloy carbides [94]. In MMn steels, carbon is one of the most effective alloying elements for decreasing the martensitic transformation temperatures (M_s and M_f) and thereby promoting the formation of retained austenite [95]. The M_s temperature can be calculated using the following newly developed empirical formula for MMn steels [96]:

$$M_s = 517 - 423C - 30.4Mn + 37Al + 82Mo - 700B \quad (1)$$

where the M_s temperature is in degree Celsius and the element contents are in wt. %. Equation (1), unlike some earlier empirical formulae, does not consider the effect of grain size on M_s ; however, this may play an important role in MMn steels, which have ultra-fine austenite grains (UFG). Garcia-Jucedá et al. [97] and Yang et al. [98] found that M_s decreased as the austenite grain size was reduced and that this tendency became stronger when the value was below 5 μm . Lee et al. [99,100] modified the empirical formula of Andrews et al. [101] with grain size to predict M_s of UFG MMn steels, but this still requires further validation. An excessive carbon content will bring with it a series of problems, such as poor plasticity and welding performance.

2. Manganese is another important alloying element in medium-Mn steel, acting as a strong austenite stabiliser [102]. After ART annealing and suitably rapid cooling, austenite with a high Mn content remains present in the microstructure at room temperature due to the low M_s temperature. Figure 9 shows an example of a continuous cooling transformation diagram for a medium-Mn steel with 5 wt. % Mn, as obtained by dilatometry [103]. The kinetics of formation of bainite are relatively slow (requiring a cooling rate of $<1 \text{ } ^\circ C \text{ s}^{-1}$) and the transformation to ferrite/pearlite is absent even under an extremely low cooling rate of $0.028 \text{ } ^\circ C \text{ s}^{-1}$, which means that transformation to other microstructures than martensite can easily be avoided by quenching. Very similar results showing such low critical cooling rates for the austenite-to-martensite transformation can be found in other investigations for MMn steels with around 5–8 wt. % Mn [104–106]. The amount of retained austenite in the MMn steel is dependent on the Mn content. For example, after ART

annealing at 650 °C for 6 h, MMn steels with Mn concentrations of 4 wt. %, 6 wt. % and 8 wt. % showed austenite volume fractions of 25%, 41% and 47%, respectively [107]. In addition, Mn is the element in MMn steels with the most important effect in decreasing the austenitic transformation temperatures (A_1 and A_3), leading to potential application in LTHS. However, an excessive amount of Mn can lead to poor weldability.

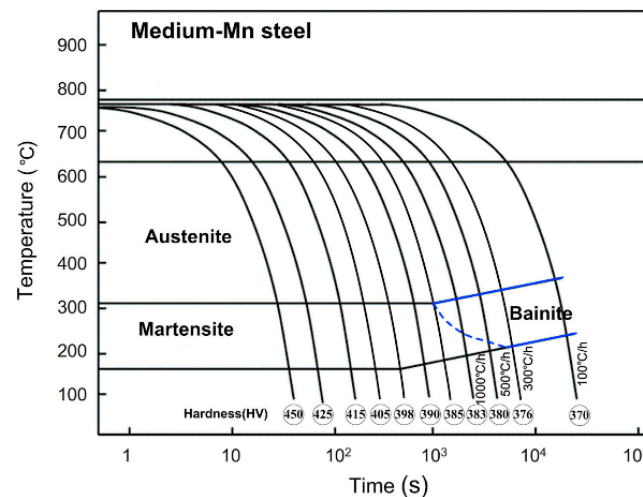


Figure 9. Continuous cooling transformation (CCT) diagram for 5Mn steel (Reproduced with permission from Elsevier [103]).

3. Silicon is a ferrite-stabilising element and is used to inhibit the precipitation of cementite and promote the partitioning of carbon into austenite during ART annealing. It does this by increasing the activation energy for cementite nucleation [108]. The addition of silicon can also enhance both strength and ductility by increasing the strain hardening rate [109]. However, an excessive silicon content can reduce the surface quality and promote the formation of a thick oxide layer.
4. Aluminium is, similarly to silicon, a ferrite stabilising element that impedes the precipitation of carbides. Additionally, an appropriate amount of Al (<0.05 wt. %) refines the grains and enhances the mechanical properties after ART annealing [108,110]. However, Al also increases the austenitic transformation temperatures and its effect is stronger than that of Mn in decreasing them. Thus, care should be taken regarding the amount added in medium-Mn steel if it is intended that LTHS be applied.

4.2.2. Production Process for Medium-Mn Steels

Figure 10a shows a general production process for a MMn steel [111–113]. After smelting and casting, the material is heated up to an elevated temperature of around 1200 °C for 1–2 h to remove defects such as gas porosity, shrinkage, hot tears and hot spots, and to homogenise the microstructure. The material is then hot rolled several times until the desired thickness of 3–5 mm is achieved; during this process, the temperature is maintained above 900 °C. The hot-rolled material is water-cooled to room temperature, then annealed at an intercritical temperature (i.e., between A_1 and A_3) for several hours until the material is softened and has a microstructure of ferrite and retained austenite. The softened material can then be cold rolled into very thin sheets (1–2 mm), giving a microstructure consisting of ferrite and strain-induced martensite with a high dislocation density. The cold-rolled material is then ART annealed. During this treatment, the highly deformed martensite first decomposes to ferrite and cementite and then the ferrite undergoes recrystallisation because of the large amount of stored energy it contains [114]. Subsequently, since the ART annealing is also carried out at an intercritical temperature, austenite nucleates, mainly on boundaries in the parent martensite substructure (lath or block) and on interfaces between ferrite and cementite [115,116]. Over a period of several minutes to

several hours, cementite is gradually dissolved, and the high concentration of Mn and C released then partitions into the newly formed austenite, while Al and Si partition out of the austenite into the ferrite. If the austenite formed during ART annealing has a high enough Mn and C content and very fine grains ($<1 \mu\text{m}$), a martensitic transformation can be avoided during subsequent quenching to room temperature (see Equation (1)).

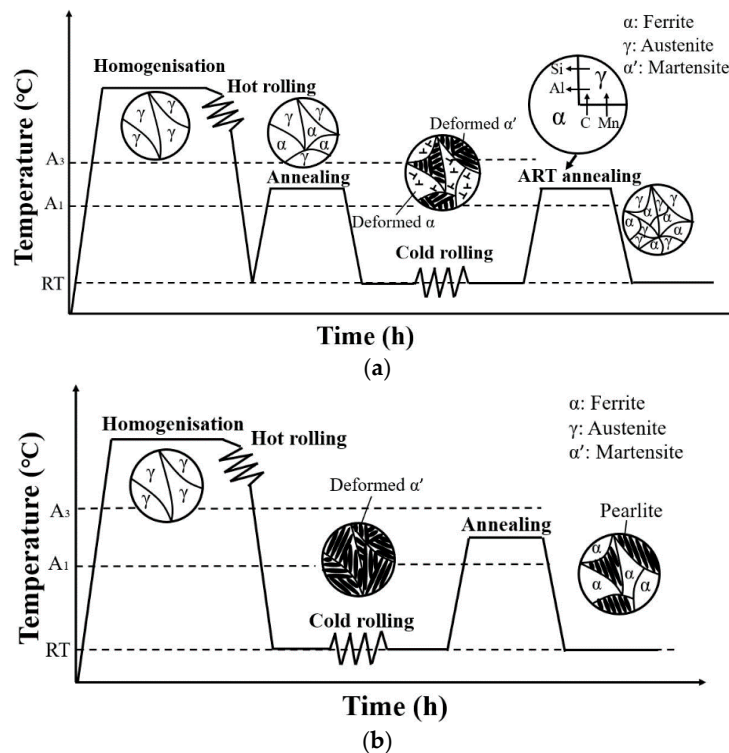


Figure 10. Schematic illustration of production processes, with evolution of microstructure, for (a) MMn steel and (b) Mn-B steel.

If the required thickness for car components of around 1–2 mm can be achieved directly by hot rolling, then the cold rolling step and subsequent ART annealing shown in Figure 10a could become unnecessary. This is because the annealing treatment after hot rolling (labelled “Annealing” in Figure 10a) is also intercritical and will result in the formation of retained austenite. However, without cold rolling, there may not be sufficient stored energy in the microstructure to promote recrystallisation, and thus grain refinement, during annealing [114]. In addition, the high dislocation density after cold rolling enables extensive pipe diffusion, giving rapid partitioning of the elements, especially Mn. This results in an acceleration in the ART process, which requires only minutes in the cold-rolled material, as compared to hours in the hot-rolled material [117].

In the conventional Mn-B hot stamping process (Figure 10b) [118,119], the annealing step between hot rolling and cold rolling is omitted because the hot-rolled material is sufficiently soft to directly undergo cold rolling due to the relatively low alloying element content. After subsequent annealing, the cold-rolled sheet is able to be coiled and has a final microstructure consisting of pearlite and ferrite with a coarse grain size of around $10 \mu\text{m}$ [120].

As shown in Figure 11a, the total cost of a single conventionally hot-stamped part can be divided into three parts: the cost of raw materials (e.g., iron ore, other ores for alloying elements), the cost of production (e.g., steelmaking, casting, hot/cold rolling and annealing) and the cost of hot stamping (e.g., heating, stamping and post-form treating). The contributions of each of these factors to the total cost are not equal and can depend on many factors, such as the shape of the part, the time of production (variations in price of raw materials and energy) and the country of production (costs of labour, transport etc. [121]). However, for the purposes of illustration, they are treated as equal in Figure 11.

Compared to conventional hot-stamping steels, MMn steels (Figure 11b) have higher raw material costs because of their higher concentration of alloying elements (Mn, Al, etc.) and higher production costs due to the additional annealing step necessary before cold rolling. However, the cost of the hot stamping process for MMn steel can be reduced with respect to conventional hot stamping of Mn-B steels. In particular, both the heating and forming temperature can be reduced by around 100–200 °C, which may not only avoid the necessity of coating to protect from oxidation and decarburisation and of shot blasting after hot stamping and the concomitant costs [103,122], but also reduce the possibility of damage to the die (lower wear rate at lower temperatures) and the repair costs [123,124]. Moreover, it is well known that Mn-B steels require a quenching rate of at least 27 °C s^{-1} to achieve a fully martensitic microstructure [125], but a very low quench rate is required for MMn steels [104,126]; hence, the requirements for the die and quenching system are not as stringent for MMn steel and the equipment cost is lower [37,70]. As a result, although the detailed production process for the hot-stamped MMn steels is still under investigation, these alloys have a great potential for total cost reduction, as shown in Figure 11b.

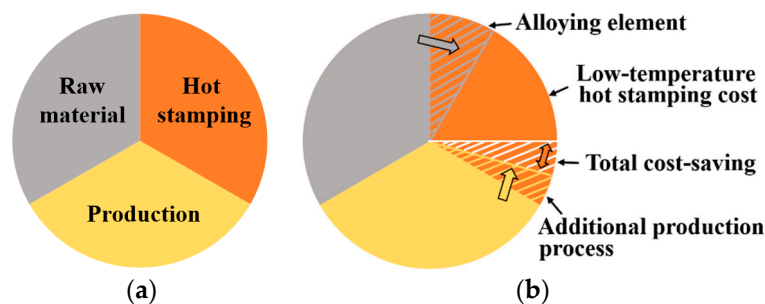


Figure 11. Schematic of estimated cost breakdown for (a) conventional Mn-B steel; (b) MMn steel.

In addition, production costs for MMn steels could possibly be reduced by directly using cold-rolled, hot-rolled or warm-rolled sheet without ART annealing as the initial state for the hot stamping process. Li et al. [122] directly used cold-rolled MMn steels as the hot-stamping material and found that the final mechanical properties of the stamped parts were similar to those of the ART-annealed material. However, the details of the effect of retained austenite (obtained after ART annealing) on the final mechanical behaviour of the hot-stamped material are still unknown and further research into this is required. As well as the ART annealing process, several other novel methods have been developed for MMn steels, such as warm rolling [127], double annealing [128] and ART annealing + Q&P [129], as shown in Figure 12a–c, respectively. All of these have been developed to further improve the mechanical properties, especially toughness, after cold forming. Their feasibility for hot stamping is as yet unknown and needs further research.

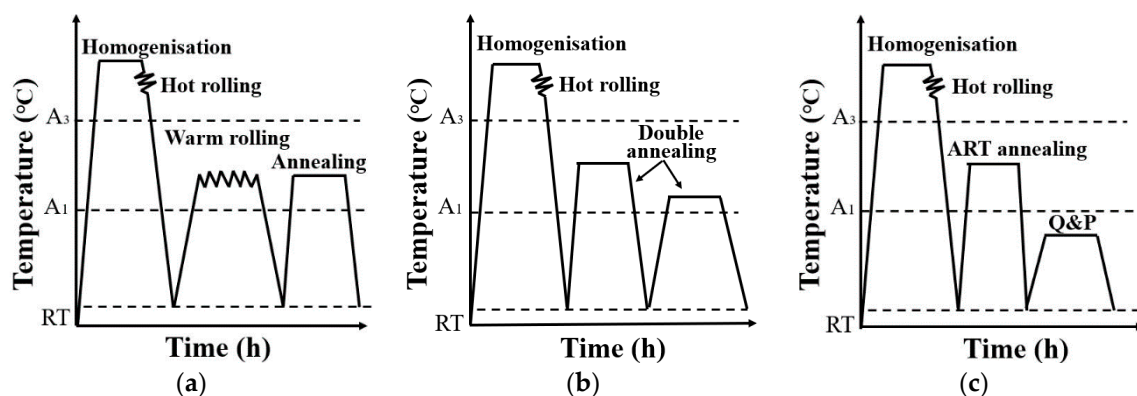


Figure 12. Other novel production processes for MMn steels: (a) Warm rolling; (b) Double annealing; (c) Q&P.

4.2.3. Strengthening Mechanism in Medium-Mn Steel

After the production process, the microstructure of medium-Mn steel is composed of multiple constituents, i.e., ferrite and retained austenite, on different length scales. Dong et al. [130] have proposed a novel control theory for microstructures that are multi-phase, multi-scale and metastable (M3). Materials with complex microstructures having M3 features can often give good combinations of strength and toughness through enhancement of the strain hardening rate and inhibition of crack nucleation and propagation during deformation and fracture [131]. MMn steels are a typical example of this, especially those with large amounts of metastable austenite. The key factor for simultaneous improvement of strength and toughness of MMn steels is to increase the strengthening rate or prolong the duration of strengthening by the metastable austenite during deformation [132]. For MMn steels after ART annealing, the metastable austenite present in the microstructure is transformed via the TRIP and/or TWIP effects with increasing strain [133,134]. One of the main factors governing the strengthening mechanism is the stacking fault energy (SFE) of the retained austenite, which depends strongly on the Mn content. For deformation at room temperature, the TRIP effect occurs preferentially in RA with <9 wt. % Mn, corresponding to an SFE lower than $18 \text{ mJ}\cdot\text{m}^{-2}$, whereas the TWIP effect occurs preferentially when the SFE is between 15 and $35 \text{ mJ}\cdot\text{m}^{-2}$, which is associated with a Mn content >15 wt. % [135,136]. The deformation temperature and austenite grain size may also influence the deformation mechanism; the TWIP effect is preferred for higher deformation temperatures and smaller grain sizes [137,138]. The strengthening rate can thus be kept high throughout the deformation of MMn steels, delaying the onset of necking and increasing the ultimate tensile strength and toughness of the material [139,140].

The martensite plates formed from retained austenite via the TRIP effect act as strong barriers against dislocation glide, thereby enhancing the strength [141]. The mechanical twinning induced in the retained austenite via the TWIP effect is not only a barrier to dislocation glide, but also provides sites for further nucleation of martensite [142]. Energy is absorbed by both types of transformations at the tip of any cracks formed, providing an obstacle to crack propagation and thus, improving the ductility. Although these strengthening mechanisms may have a significant influence on the mechanical properties, details of the effects and their interactions have not yet been investigated in depth, and much research is still required into the mechanical behaviour of MMn steels in cold forming. The evolution of retained austenite during hot stamping and its effect on the deformation mechanism under conditions of high- or room-temperature deformation are also not well understood.

5. Application of Low-Temperature Hot Stamping Process in Medium-Mn Steel

As a result of the advanced features of medium-Mn steels, the research direction has gradually shifted in recent years from cold forming to low-temperature hot stamping. A general schematic diagram of the process is shown in Figure 13. The soaking (austenitisation) temperature depends on the A_3 temperature, which is in turn related to the chemical composition of the material. It has usually been set at 30–80 °C above A_3 in most of the research conducted so far, e.g., [103,122,126,143]. The average austenitisation temperature is thus around 100–200 °C lower than that in the traditional hot stamping process for boron steel. After soaking, the heated material is rapidly transferred to the die and stamped and quenched as in the conventional procedure. Some retained austenite may be present at room temperature, but most of the microstructure is martensitic [144–146]. However, microstructural evolution during the LTHS process has not yet been studied in depth, nor has its effect on forming behaviour and final mechanical behaviour been investigated.

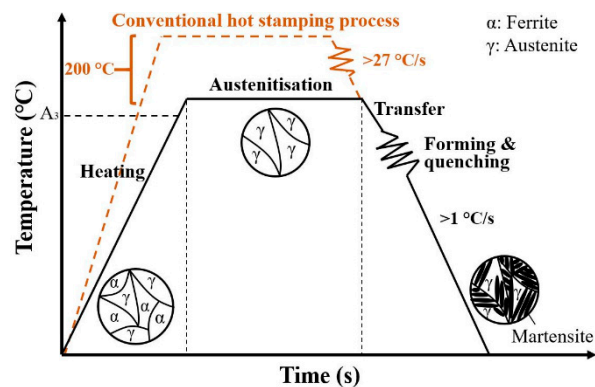


Figure 13. Schematic representation of low-temperature hot stamping of Medium-Mn steel and its microstructural evolution. The conventional hot stamping process is shown with dashed lines for comparison.

A number of examples of process conditions and final mechanical properties of low-temperature hot stamped MMn steels with different element contents are presented in Table 2. Chang et al. [126] investigated the application of LTHS to ART-annealed MMn steels. They determined the optimal process windows by which the best formability and final mechanical properties could be obtained. These were 780–840 °C for 4–7 min for austenitisation, and 450–500 °C for stamping; the optimal cooling rate was 10–60 °C s⁻¹. These conditions can be achieved with a traditional hot stamping production line. After stamping, the ultimate tensile strength was around 1400 MPa with a total elongation of 11.8%. Wang et al. [143] suggested that an austenitising temperature of 800 °C was sufficient for the complete austenitisation of 5Mn steel and reduced oxidation and decarburisation. This low-temperature hot stamped material had fine microstructure and attained an ultimate tensile strength of 1500 MPa with an elongation of 10%. Based on this, Li et al. [103] further investigated 5Mn steel after LTHS. They found that unlike in hot-stamped 22MnB5 steel, the M_s temperature was not sensitive to the forming temperature and pressure, resulting in even distributions of microstructure and mechanical properties. Pan et al. [145] investigated the tensile behaviour of low-temperature hot stamped 5.6Mn steel after warm rolling without ART annealing. An excellent UTS × TE product of around 27.5 GPa·% was obtained in this material. The reason for such good mechanical properties is not yet well understood, but it may be related to a higher degree of M3 features in the microstructure, which was observed to be of an ultrafine and multiphase character. Lu et al. [146] examined the effect of post-processing on the microstructure and mechanical properties of low-temperature hot stamped 7.0Mn steel. A process of baking at 170 °C for 20 min was introduced after the whole stamping process to re-partition the carbon into the retained austenite. This was found to improve the ductility significantly by enabling continuous occurrence of the TRIP or TWIP effects during deformation. As a result of this baking, the total elongation was increased from around 3% to 11.7%. Hou et al. [144] and Li et al. [122] have also examined the effect of post-processing on the mechanical behaviour of cold-rolled MMn steel after LTHS. After subsequent baking at 170 °C for 20 min, very high tensile strengths of 1805 MPa and 1700 MPa and total elongations of 16% and 11.8% were obtained in 7.5Mn and 6.5Mn steels, respectively. The cost of the additional baking process need not be included in cost calculations because baking can be combined with paint tempering in real production lines. There is the possibility of not only an improvement in mechanical properties, but also a reduction in cost if the ART annealing process can be omitted. However, more research is required to understand the evolution of microstructure and its effect on final performance after hot stamping before this experimental ART-free process can be used in real applications.

Table 2. Reported tensile properties of some low-temperature hot stamped MMn steels.

Ref.	Initial State	Austenitisation Condition	YS (MPa)	UTS (MPa)	TE (%)	UTS × TE (GPa-%)
[126]	ART-annealed	810 °C, 5 min	1220	1418	11.8	16.7
[103,143]	ART-annealed	800 °C, 5 min	1050	1520	10–11.3	15.2–17.2
[145]	Warm-rolled	800 °C, 8 min	852	1717	16	27.5
[146]*	ART-annealed	760 °C, 5 min	1080	1565	11.7	18.3
[144]*	Cold-rolled	780 °C, 5 min	1400	1805	16	28.9
[122]*	Cold-rolled	750 °C, 5 min	1420	1700	11.8	20.1

* Post-form baking was performed. ART: austenite reverse transformation.

Oxidation and decarburisation are unavoidable when uncoated steels are exposed to air at elevated temperature during the hot stamping process. The oxide layer formed by reaction between the outer surface of the sheet and atmospheric oxygen must be removed after hot stamping and has a deleterious effect on the dimensional accuracy of the product [147]. The inner decarburisation layer is caused by the loss of carbon and not only reduces the strength, but also increases the shear rate, which promotes crack growth and reduces the fatigue resistance of the hot-stamped material [148,149]. In addition, both the oxidation and the decarburisation layer affect the heat transfer during die quenching, decreasing productivity. It can be seen in Figure 14 that decarburisation layers of over 100 µm in depth are formed in the surface microstructure of a hot stamped 22MnB5 steel austenitised for 5 min at 920 °C (Figure 14a [103]) and around 40–50 µm heated at 950 °C for 5 min even under a protective nitrogen atmosphere (Figure 14c [143]). In contrast, only an extremely thin decarburisation layer was observed in an MMn steel after austenitisation at 800 °C for 5 min both without (Figure 14b [103]) and with (Figure 14d [143]) a protective nitrogen atmosphere. If the formation of this layer can be avoided, this will provide a considerable saving in both tooling and coating costs.

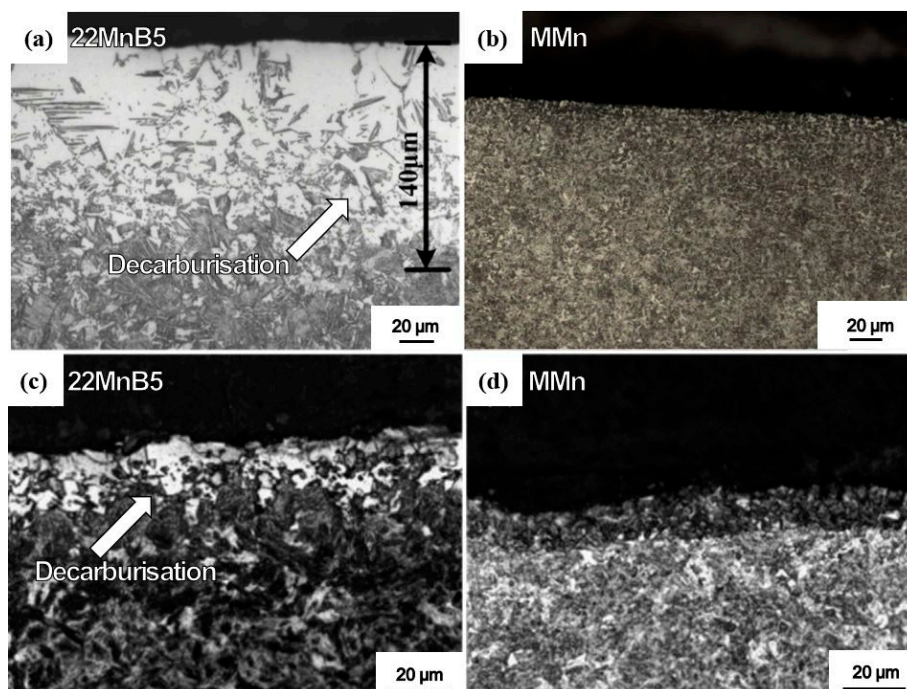


Figure 14. Optical microscopy images of cross-sectional microstructure of the surface region, showing the oxidation and decarburisation layers for: (a,c) 22MnB5 steel; (b,d) MMn steel; the samples in (c,d) are heated under a protective nitrogen atmosphere (Adapted with permission from Elsevier, John Wiley and Sons [103,143]).

It has been shown experimentally in a real stamped automotive part that uniform tensile properties can be obtained through LTHS [126]. Measurements of tensile strength, yield strength and total elongation from various positions in the part are given in Figure 15. These results showed that the

variation in each tensile property over all measurement locations did not exceed 5%, demonstrating an even distribution of mechanical properties across the part [126]. Zheng et al. [150] studied the effect of various hot forming parameters on the formability of MMn steel (5 wt. % Mn) and 22MnB5 steel based on square-cup deep drawing, both numerically and experimentally. Their results demonstrated that the strain rate ($0.01\text{--}1.0\text{ s}^{-1}$) had a strong influence in the 22MnB5, but only a weak influence in the MMn steel. The mechanical behaviour during hot forming in the MMn steel was also less sensitive to deformation temperature than in the 22MnB5 steel. The MMn steel had, overall, a better formability in deep drawing during the hot stamping process with a more uniform thickness and distribution of martensitic microstructure. The reason for this improved uniformity of distribution has not yet been clarified, but it was shown that MMn steels give favourable results when they are used to produce complex-shaped automobile structure components by LTHS.

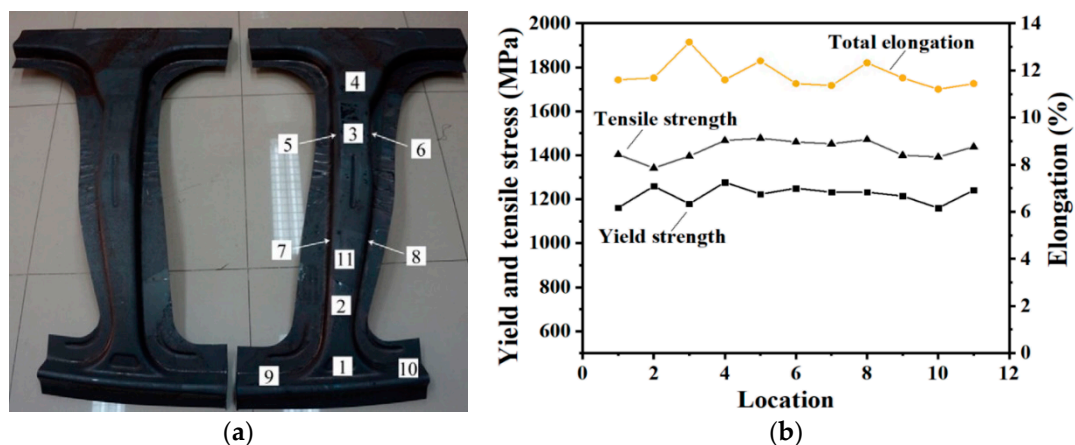


Figure 15. Low-temperature hot stamping of MMn steel component: (a) Low-temperature hot stamped B-pillar [126]; The numbers show the positions on the hot stamped B-pillar selected for testing of mechanical properties. (b) Mechanical properties (tensile strength, yield strength and elongation) at corresponding locations [126]. Adapted from [126], with permission from Elsevier, 2020.

Overall, MMn steels have many merits over alternative materials when applying hot stamping processes, including reduced cost, improved productivity, a good combination of strength and ductility and good formability and hardenability. However, research in this field is currently still insufficient for commercialisation and industrialisation. Further research effort is required in order to develop low-temperature hot stamped products and provide a total technical solution for part manufacturing and use. In addition, an understanding of the evolution of microstructure and, in particular, retained austenite during the process, and the role of this in the strengthening mechanism and final performance, are also important.

6. Conclusions and Prospects

A detailed review of recent developments in the field of hot stamping technology has been presented in this paper. In recent years, in order to improve the stamping process from the point of view of cost, productivity and final performance of stamped parts, research has focused on improvements to the hot-stamping process and, in particular, on reducing the temperature at which part or all of the process is carried out. Great progress has been made, building a foundation for further application of hot- or warm-stamped components in the automotive industry. Some conclusions and prospects can be summarised as follows:

- (1) Many advanced techniques have been developed to support improvements in the hot stamping process including cost savings, reduction in cycle time and enhancement in tensile properties of hot-stamped components. Reducing the temperature of the process has been shown to be one of the most advantageous approaches, with excellent prospects.

- (2) Low-temperature approaches for conventional steels involve reducing the heating and forming temperatures (warm forming) or just the forming temperature (low-temperature hot stamping). The feasibility of using a lower heating temperature has been investigated with conventional hot stamping materials. Although the cost and productivity and the toughness of the components are thereby improved, the strengths attained are lower than those achieved by conventional hot stamping. For applications where high toughness is more important than high strength, components formed using this approach may be an acceptable replacement for conventionally hot-stamped parts. Lowering forming temperatures only is another approach to keep the ultra-high strength while shortening the cooling cycle time, increasing the lifetime of dies and improving the formability. However, since the austenitising temperature is still high, similarly to conventional hot stamping, the high cost of preventing oxidation and decarburisation, as well as insufficient ductility, are still a problem.
- (3) In recent years, third-generation advanced high strength steels have been developed rapidly; these have both ultra-high strength and high toughness, enabling them to meet most of the requirements of automobile applications with lower alloying costs than second-generation steels. Medium-Mn (MMn) steels are a typical example of third-generation steels, and great progress has been made in applying them in cold forming processes. Their low austenitisation temperatures have resulted in much research attention to this class of material as a replacement for conventional Mn-B steel in hot stamping processes.
- (4) The feasibility of low-temperature hot stamping techniques with MMn steels has been investigated and positive results have been reported. Besides the low cost and high productivity, the mechanical properties can be better than those of conventional boron steels. In addition, the formability and hardenability are also excellent, which is advantageous for producing components with complex shapes.
- (5) Further research is necessary in the field of low-temperature hot stamping of MMn steel to facilitate industrial application and replace the traditional boron steels. Experiments have shown that it may be possible to further reduce the manufacturing cycle time, and thus the production cost, in MMn steel by eliminating the ART annealing step. However, the microstructural mechanisms governing the effect of retained austenite obtained in the ART annealing process on the forming behaviour during hot stamping and on the final tensile properties after hot stamping are still not well understood. It is important to gain a comprehensive understanding of the relationship between processing conditions, microstructure and mechanical behaviour in these steels in order to control process speeds and the quality of components.

Author Contributions: C.T.: methodology, investigation, visualization, writing—original draft preparation; Q.R.: investigation, writing—review and editing; V.A.Y.: methodology, writing—review and editing; X.L.: project administration, writing—review and editing; J.L.: methodology, supervision; G.Z.: conceptualization, funding acquisition; Z.S.: conceptualization, writing—review and editing, supervision, funding acquisition. All authors have read and agreed to the published version of the manuscript.

Funding: This research was funded by the Shougang Group, China with the project number MESM_P72577.

Acknowledgments: The funding support from Shougang Research Institute of Technology, Shougang Group, China for this research is much appreciated. The research was performed at the Shougang–Imperial Lab for Lightweight Steel-Based Systems for Impact Resistant Automotive Applications at Imperial College London.

Conflicts of Interest: The authors declare that there are no conflict of interest.

References

1. Kiani, M.; Gandikota, I.; Rais-Rohani, M.; Motoyama, K. Design of lightweight magnesium car body structure under crash and vibration constraints. *J. Magnes. Alloys* **2014**, *2*, 99–108. [[CrossRef](#)]
2. Berglund, G. The history of hardening of boron steel in northern Sweden. In Proceedings of the 1st International Conference on Hot Sheet Metal. Forming of High-Performance Steel, Kassel, Germany, 22–24 October 2008; pp. 175–177.

3. Karbasian, H.; Tekkaya, A.E. A review on hot stamping. *J. Mater. Process. Technol.* **2010**, *210*, 2103–2118. [[CrossRef](#)]
4. Advanced High Strength Steel Technologies in the 2016 Volvo XC90. 2017. Available online: <https://www.sasft.org/-/media/files/autosteel/great-designs-in-steel/gdis-2016/track-2---volvo-xc90.ashx> (accessed on 20 September 2020).
5. Lightweight Door Ring Concepts Using Hot Stamped Laser Welded Blanks. 2014. Available online: <https://www.sasft.org/-/media/files/autosteel/great-designs-in-steel/gdis-2014/gagan-tandon---amfb.ashx> (accessed on 20 September 2020).
6. Pentera, L.; Pierschel, N. Thermo-mechanical interactions in hot stamping. In Proceedings of the CIRP sponsored Conference on Thermal Issues in Machine Tools, Dresden, Germany, 21–23 March 2018.
7. Fujisawa, T.; Hamada, S.; Koga, N.; Sasaki, D.; Tsuchiyama, T.; Nakada, N.; Takashima, K.; Ueda, M.; Noguchi, H. Proposal for an engineering definition of a fatigue crack initiation unit for evaluating the fatigue limit on the basis of crystallographic analysis of pearlitic steel. *Int. J. Fract.* **2013**, *185*, 17–29. [[CrossRef](#)]
8. Chang, Y.; Li, G.; Wang, C.; Li, X.; Dong, H. Effect of quenching and partitioning with hot stamping on martensite transformation and mechanical properties of AHSS. *J. Mater. Eng. Perform.* **2015**, *24*, 3194–3200. [[CrossRef](#)]
9. Merklein, A.; Lechler, J. Investigation of the thermo-mechanical properties of hot stamping steels. *J. Mater. Process. Technol.* **2006**, *177*, 452–455. [[CrossRef](#)]
10. Naderi, M.; Ketabchi, M.; Abbasi, M.; Bleck, W. Analysis of microstructure and mechanical properties of different high strength carbon steels after hot stamping. *J. Mater. Process. Technol.* **2011**, *211*, 1117–1125. [[CrossRef](#)]
11. Merklein, M.; Wieland, M.; Lechner, M.; Bruschi, S.; Ghiotti, A. Hot stamping of boron steel sheets with tailored properties: A review. *J. Mater. Process. Technol.* **2016**, *228*, 11–24. [[CrossRef](#)]
12. Taylor, T.; Clough, A. Critical review of automotive hot-stamped sheet steel from an industrial perspective. *Mater. Sci. Technol.* **2018**, *34*, 809–861. [[CrossRef](#)]
13. Ganapathy, M.; Li, N.; Lin, J.; Bhattacharjee, D. Investigation of a new hot stamping process with improved formability and productivity. *Procedia Eng.* **2017**, *207*, 771–776. [[CrossRef](#)]
14. Hu, B.; Luo, H.W.; Yang, F.; Dong, H. Recent progress in medium-Mn steels made with new designing strategies, a review. *J. Mater. Sci. Technol.* **2017**, *33*, 1457–1464. [[CrossRef](#)]
15. Naderi, M.; Ketabchi, M.; Abbasi, M.; Bleck, W. Semi-hot stamping as an improved process of hot stamping. *J. Mater. Sci. Technol.* **2011**, *27*, 369–376. [[CrossRef](#)]
16. Choi, H.; Lim, W.; Seo, P.; Kang, C.; Kim, B. Softening method for reducing trimming load and improving tool wear resistance in cutting of a hot stamped component. In Proceedings of the international conference on technology of plasticity, Technology of plasticity, Aachen, Germany, 25–30 September 2011; pp. 419–422.
17. Kim, P.; Chun, M.; Yi, J.; Moon, Y. Pass schedule algorithms for hot open die forging. *J. Mater. Process. Technol.* **2002**, *130*, 516–523. [[CrossRef](#)]
18. Lehmann, H. Developments in the field of Schwartz heat treatment furnaces for press hardening industry. In Proceedings of the 3rd International Conference on Hot Sheet Metal Forming of High-Performance Steel, Kassel, Germany, 13–17 June 2010; pp. 171–180.
19. Mori, K. Smart hot stamping of ultra-high strength steel parts. *Trans. Nonferrous Met. Soc. China* **2012**, *22*, 496–503. [[CrossRef](#)]
20. Mori, K.; Bariani, P.F.; Behrens, B.A.; Brosius, A.; Bruschi, S.; Maeno, T.; Merklein, M.; Yanagimoto, J. Hot stamping of ultra-high strength steel parts. *CIRP Ann. Manuf. Technol.* **2017**, *66*, 755–777. [[CrossRef](#)]
21. Zhang, Z.; Jia, X.; Li, X.; Zhao, Y. Hot stamping of boron alloy steels using resistance heating. In Proceedings of the 2nd International Conference on Civil, Materials and Environmental Sciences, London, UK, 13–14 March 2015; pp. 362–365.
22. Kolleck, R.; Veit, R.; Merklein, M.; Lechler, J.; Geiger, M. Investigation on induction heating for hot stamping of boron alloyed steels. *CIRP Ann. Manuf. Technol.* **2009**, *58*, 275–278. [[CrossRef](#)]
23. Kim, D.K.; Woo, Y.Y.; Park, K.S.; Sim, W.J.; Moon, Y.H. Advanced induction heating system for hot stamping. *Int. J. Adv. Manuf. Technol.* **2018**, *99*, 583–593. [[CrossRef](#)]
24. Vibrans, T.; Malek, R.; Kotzian, M.; Vogt, C.; Langejürgen, M. Development of an induction heating heating device for heating shaped blanks. *Heat Process.* **2016**, *3*, 37–42.

25. Ploshikhin, V.; Prihodovsky, A.; Kaiser, J.; Brisping, R.; Linder, H.; Lengsdorf, C. New heating technology for furnace-free press hardening process. In Proceedings of the Tools and Technologies for Processing Ultra-High Strength Materials, Graz, Austria, 19–21 September 2011.
26. Ploshikhin, V.; Prihodovsky, A.; Kaiser, J.; Skutella, L. Contact heating—New heating technology for heat treatment and hot forming. In Proceedings of the Tools and Technologies for Processing Ultra High Strength Materials, Graz, Austria, 19–20 September 2013.
27. Aikawa, S. Far-Infrared Radiation Heating Furnace for Steel Sheet for Hot Stamping. U.S. Patent 20170175218A1, 6 December 2017.
28. Kuwayama, S. Far-Infrared Radiation Multi-Stage Type Heating Furnace for Steel Sheets for Hot Stamping. U.S. Patent 20170159141A1, 8 June 2017.
29. Lee, E.H.; Hwang, J.S.; Lee, C.W.; Yang, D.Y.; Yang, W.H. A local heating method by near-infrared rays for forming of non-quenchable advanced high-strength steels. *J. Mater. Process. Technol.* **2014**, *214*, 784–793. [[CrossRef](#)]
30. Lee, E.H.; Yoon, J.W.; Yang, D.Y. Study on springback from thermal-mechanical boundary condition imposed to V-bending and L-bending processes coupled with infrared rays local heating. *Int. J. Mater. Form.* **2018**, *11*, 417–433. [[CrossRef](#)]
31. Hot Stamping Presses with PCH Flex Technology. 2015. Available online: <https://www.schulergroup.com/major/us/technologien/produkte/formhaerteanlagen/index.html> (accessed on 20 September 2020).
32. Vollmer, R.; Palm, C. Improving the quality of hot stamping parts with innovative press technology and inline process control. *J. Phys. Conf. Ser.* **2017**, *896*, 012050. [[CrossRef](#)]
33. Palm, C.; Vikkner, R.; Aspacher, J.; Gharbi, M. Increasing performance of hot stamping systems. *Procedia Eng.* **2017**, *207*, 765–770. [[CrossRef](#)]
34. Maeno, T.; Mori, K.I.; Fujimoto, M. Improvements in productivity and formability by water and die quenching in hot stamping of ultra-high strength steel parts. *CIRP Ann.* **2015**, *64*, 281–284. [[CrossRef](#)]
35. Shan, Z.; Zhang, M.; Jiang, C.; Xu, Y.; Rong, W. Basic study on die cooling system of hot stamping process. In Proceedings of the International Conference on Advanced Technology of Design and Manufacture, IET, Beijing, China, 23–25 November 2010; pp. 65–68.
36. Valls, I.; Casas, B.; Rodriguez, N.; Paar, U. Benefits from using high thermal conductivity tool steels in the hot forming of steels. In Proceedings of the International Conference Hot Forming of Steels and Products Properties, Grado, Italy, 13–16 September 2009.
37. Lim, W.; Choi, H.; Ahn, S.; Kim, B. Cooling channel design of hot stamping tools for uniform high-strength components in hot stamping process. *Int. J. Adv. Manuf. Technol.* **2014**, *70*, 1189–1203. [[CrossRef](#)]
38. Xu, Y.; Shan, Z.D. Design parameter investigation of cooling systems for UHSS hot stamping dies. *Int. J. Adv. Manuf. Technol.* **2014**, *70*, 257–262.
39. Lei, C.; Cui, J.; Xing, Z.; Fu, H.; Zhao, H. Investigation of cooling effect of hot-stamping dies by numerical simulation. *Phys. Procedia* **2012**, *25*, 118–124. [[CrossRef](#)]
40. Li, S.; Zhou, L.H.; Wu, X.C.; Zhang, Y.; Li, J.W. The influence of thermal conductivity of die material on the efficiency of hot-stamping process. *J. Mater. Eng. Perform.* **2016**, *25*, 4848–4867. [[CrossRef](#)]
41. Clarke, A.J.; Speer, J.G.; Matlock, D.K.; Rizzo, F.C.; Edmonds, D.V.; Santofimia, M.J. Influence of carbon partitioning kinetics on final austenite fraction during quenching and partitioning. *Scr. Mater.* **2009**, *61*, 149–152. [[CrossRef](#)]
42. Edmonds, D.V.; He, K.; Rizzo, F.C.; De Cooman, B.C.; Matlock, D.K.; Speer, J.G. Quenching and partitioning martensite—A novel steel heat treatment. *Mater. Sci. Eng. A* **2006**, *438*, 25–34. [[CrossRef](#)]
43. Speer, J.; Matlock, D.K.; De Cooman, B.C.; Schroth, J.G. Carbon partitioning into austenite after martensite transformation. *Acta Mater.* **2003**, *51*, 2611–2622. [[CrossRef](#)]
44. Speer, J.G.; Edmonds, D.V.; Rizzo, F.C.; Matlock, D.K. Partitioning of carbon from supersaturated plates of ferrite, with application to steel processing and fundamentals of the bainite transformation. *Curr. Opin. Solid St. M.* **2004**, *8*, 219–237. [[CrossRef](#)]
45. Oldenburg, M. Warm forming of steels for tailored microstructure. In *Encyclopedia of Thermal Stresses*; Hetnarski, R.B., Ed.; Springer: Dordrecht, The Netherlands, 2014; pp. 6469–6479.
46. Laumann, T.; Pfestorf, M.; Beil, A.; Geiger, M.; Merklein, M. Crash behaviour of various modern steels exposed to high deformation rates. *Key Eng. Mater.* **2007**, *344*, 151–158. [[CrossRef](#)]

47. Mori, K.; Maeno, T.; Mongkolkaji, K. Tailored die quenching of steel parts having strength distribution using bypass resistance heating in hot stamping. *J. Mater. Process. Technol.* **2013**, *213*, 508–514. [[CrossRef](#)]
48. George, R.; Bardelcik, A.; Worswick, M.J. Hot forming of boron steels using heated and cooled tooling for tailored properties. *J. Mater. Process. Technol.* **2012**, *212*, 2386–2399. [[CrossRef](#)]
49. Yogo, Y.; Kurato, N.; Iwata, N. Investigation of hardness change for spot welded tailored blank in hot stamping using CCT and deformation-CCT diagrams. *Metall. Mater. Trans. A* **2018**, *49a*, 2293–2301. [[CrossRef](#)]
50. Yun, S.; Lee, S.H.; Song, K.S.; Cho, W.; Kim, Y. Performance improvement of tailored die quenching using material combinations with phase change material in hot stamping. *Int. J. Heat Mass Transfer.* **2020**, *161*, 120286. [[CrossRef](#)]
51. Kim, C.; Kang, M.J.; Park, Y.D. Laser welding of Al-Si coated hot stamping steel. *Procedia. Eng.* **2011**, *10*, 2226–2231. [[CrossRef](#)]
52. Tajul, L.; Maeno, T.; Kinoshita, T.; Mori, K.I. Successive forging of tailored blank having thickness distribution for hot stamping. *Int. J. Adv. Manuf. Technol.* **2017**, *89*, 3731–3739. [[CrossRef](#)]
53. Han, X.H.; Zhong, Y.Y.; Yang, K.; Cui, Z.S.; Chen, J. Application of hot stamping process by integrating quenching and partitioning heat treatment to improve mechanical properties. *Procedia Eng.* **2014**, *81*, 1737–1743. [[CrossRef](#)]
54. Zinsaz-Borujerdi, A.; Zarei-Hanzaki, A.; Abedi, H.R.; Karam-Abian, M.; Ding, H.; Han, D.; Kheradmand, N. Room temperature mechanical properties and microstructure of a low alloyed TRIP-assisted steel subjected to one-step and two-step quenching and partitioning process. *Mater. Sci. Eng. A* **2018**, *725*, 341–349. [[CrossRef](#)]
55. Liu, H.P.; Jin, X.J.; Dong, H.; Shi, J. Martensitic microstructural transformations from the hot stamping, quenching and partitioning process. *Mater. Charact.* **2011**, *62*, 223–227. [[CrossRef](#)]
56. Liu, H.P.; Lu, X.W.; Jin, X.J.; Dong, H.; Shi, J. Enhanced mechanical properties of a hot stamped advanced high-strength steel treated by quenching and partitioning process. *Scr. Mater.* **2011**, *64*, 749–752. [[CrossRef](#)]
57. Zhu, B.; Zhu, J.; Wang, Y.A.; Rolfe, B.; Wang, Z.J.; Zhang, Y.S. Combined hot stamping and Q&P processing with a hot air partitioning device. *J. Mater. Process. Technol.* **2018**, *262*, 392–402.
58. Yilmaz, I.; Kaftanoglu, B.; Hacaloglu, T.; Kilickan, M. Integration of press hardening with codling trimming. In Proceedings of the 5th International Conference on Accuracy in Forming Technology, Chemnitz, Germany, 10–11 November 2015; pp. 105–117.
59. Mori, K.; Maeno, T.; Fuzisaka, S. Punching of ultra-high strength steel sheets using local resistance heating of shearing zone. *J. Mater. Process. Technol.* **2012**, *212*, 534–540. [[CrossRef](#)]
60. So, H.; Fassmann, D.; Hoffmann, H.; Golle, R.; Schaper, M. An investigation of the blanking process of the quenchable boron alloyed steel 22MnB5 before and after hot stamping process. *J. Mater. Process. Technol.* **2012**, *212*, 437–449. [[CrossRef](#)]
61. Mori, K.; Maki, S.; Tanaka, Y. Warm and hot stamping of ultra high tensile strength steel sheets using resistance heating. *CIRP Ann. Manuf. Technol.* **2005**, *54*, 209–212. [[CrossRef](#)]
62. Mori, K.; Abe, Y.; Miyazawa, S. Warm stamping of ultra-high strength steel sheets at comparatively low temperatures using rapid resistance heating. *Int. J. Adv. Manuf. Technol.* **2020**, *108*, 3885–3891. [[CrossRef](#)]
63. Li, N.; Li, X.; Dry, D.; Dean, T.; Lin, J.; Balint, D. Investigation on the mechanical properties of as-formed boron steels for optimizing process strategies in hot stamping. In Proceedings of the 14th International Conference of Metal Forming, Krakow, Poland, 16–19 September 2012.
64. Mu, Y.H.; Wang, B.Y.; Zhou, J.; Huang, X.; Li, X.T. Hot stamping of Boron steel using partition heating for tailored properties: Experimental trials and numerical analysis. *Metall. Mater. Trans. A* **2017**, *48a*, 5467–5479. [[CrossRef](#)]
65. Mu, Y.H.; Wang, B.Y.; Zhou, J.; Kang, Y.; Li, X.T. Heating parameters optimization of hot stamping by partition heating for tailored properties. *ISIJ Int.* **2017**, *57*, 1442–1450. [[CrossRef](#)]
66. Fridman, G.L. Use of roller-hearth and walking-beam furnaces in powder metallurgy abroad. *Sov. Power Metall. Met. Ceram.* **1968**, *7*, 583–585. [[CrossRef](#)]
67. Oh, J.; Han, U.; Park, J.; Lee, H. Numerical investigation on energy performance of hot stamping furnace. *Appl. Therm. Eng.* **2019**, *147*, 694–706. [[CrossRef](#)]
68. Hance, B.M. Advanced high-strength steel (AHSS) performance level definitions and targets. *SAE Int. J. Mater. Manuf.* **2018**, *11*, 505–516. [[CrossRef](#)]

69. Sun, Y.; Wang, K.; Politis, D.; Chen, G.; Wang, L. An experimental investigation on the ductility and post-form strength of a martensitic steel in a novel warm stamping process. *J. Mater. Process. Technol.* **2020**, *275*, 116387. [[CrossRef](#)]
70. Hoffmann, H.; So, H.; Steinbeiss, H. Design of hot stamping tools with cooling system. *CIRP Ann.* **2007**, *56*, 269–272. [[CrossRef](#)]
71. Hardell, J.; Pelcastre, L.; Prakash, B. High-temperature friction and wear characteristics of hardened ultra-high-strength boron steel. *Part J J. Eng. Tribol.* **2010**, *224*, 1139–1151. [[CrossRef](#)]
72. Balint, D.; Dean, T.A.; Lin, J. Method of Forming Parts from Sheet Steel. U.S. Patent 20140352388A1, 4 December 2014.
73. Ota, E.; Yogo, Y.; Iwata, T.; Iwata, N.; Ishida, K.; Takeda, K. Formability improvement technique for heated sheet metal forming by partial cooling. *Key Eng. Mater.* **2014**, *622–623*, 279–283. [[CrossRef](#)]
74. Verloop, W.C.; Van, G.M.J.; Van, T.R.T.; Hensen, G.C. Method to Produce a Hot Formed Part, and Part thus Formed. W.O. Patent 2012097976A1, 26 July 2012.
75. Yokoi, T.; Yamada, T.; Kawano, O. Hot Rolled Steel Sheet and Method for Production Thereof. E.P. Patent 2103697A4, 1 May 2015.
76. Okita, K.; Naitou, J.; Ikeda, S. Press-Forming Product Manufacturing Method and Press-Forming Facility. U.S. Patent 9469891B2, 18 October 2016.
77. Becker, J.U.; Bian, J.; Heller, T.; Schoenenberg, R.; Thiessen, R.G.; Zeizinger, S.; Rieger, T.; Bulters, O. High-Strength Flat Steel Product and Method for Producing Same. W.O. Patent 2012156428A1, 22 November 2017.
78. Ganapathy, M.; Li, N.; Lin, J.; Abspoel, M.; Bhattacharjee, D. Experimental investigation of a new low-temperature hot stamping process for boron steels. *Int. J. Adv. Manuf. Technol.* **2019**, *105*, 669–682. [[CrossRef](#)]
79. Ganapathy, M.; Li, N.; Lin, J.; Bhattacharjee, D. A feasibility study on warm forming of an as-quenched 22MnB5 boron steel. *Int. J. Lightweight Mater. Manuf.* **2020**, *3*, 277–283. [[CrossRef](#)]
80. Perlade, A.; Antoni, A.; Besson, R.; Caillard, D.; Callahan, M.; Emo, J.; Gourgues, A.F.; Maugis, P.; Mestrallet, A.; Thuinet, L.; et al. Development of 3rd generation Medium Mn duplex steels for automotive applications. *Mater. Sci. Technol.* **2019**, *35*, 204–219. [[CrossRef](#)]
81. Taub, A.; Luo, A. Advanced lightweight materials and manufacturing processes for automotive applications. *MRS Bull.* **2015**, *40*, 1045–1054. [[CrossRef](#)]
82. AHSS 101: The Evolving Use of Advanced High-Strength Steels for Automotive Applications. 2011. Available online: <https://www.steel.org/~{}|/media/Files/Autosteel/Research/AHSS/AHSS%20101%20%20The%20Evolving%20Use%20of%20Advanced%20HighStrength%20Steels%20for%20Automotive%20Applications%20%20lr.pdf?la=en> (accessed on 20 September 2020).
83. Jin, X.; Gong, Y.; Han, X.; Du, H.; Ding, W.; Zhu, B.; Zhang, Y.; Feng, Y.; Ma, M.; Liang, B.; et al. A review of current state and prospect of the manufacturing and application of advanced hot stamping automobile steels. *Acta Metall. Sin.* **2020**, *56*, 411–428.
84. Matlock, D.K.; Speer, J. Design considerations for the next generation of advanced high strength sheet steels. In Proceedings of the 3rd International Conference on Structures and Steels, Seoul, Korea, August 2006; pp. 774–781. Available online: https://www.researchgate.net/publication/287547477_Design_considerations_for_the_next_generation_of_advanced_high_strength_sheet_steels (accessed on 30 October 2020).
85. Galan, J.; Samek, L.; Verleysen, P.; Verbeken, K.; Houbaert, Y. Advanced high strength steels for automotive industry. *Rev. Metal.* **2012**, *48*, 118–131. [[CrossRef](#)]
86. Cao, W.; Shi, J.; Wang, C.; Wang, C.; Xu, L.; Wang, M.; Weng, Y.; Dong, H. The 3rd generation automobile sheet steels presenting with ultrahigh strength and high ductility. In *Advanced Steels: The Recent Scenario in Steel Science and Technology*; Weng, Y., Dong, H., Gan, Y., Eds.; Springer: Berlin/Heidelberg, Germany, 2011; pp. 209–227.
87. Rizzo, F.C.; Martins, A.R.; Speer, J.G.; Matlock, D.K.; Clarke, A.; De Cooman, B.C. Quenching and partitioning of Ni-added high strength steels. *Mater. Sci. Forum* **2007**, *539–543*, 4476–4481. [[CrossRef](#)]
88. Wang, C.; Chang, Y.; Yang, J.; Cao, W.; Dong, H.; Wang, Y. Work hardening behavior and stability of retained austenite for quenched and partitioned steels. *J. Iron Steel Res. Int.* **2016**, *23*, 130–137. [[CrossRef](#)]
89. Yang, F.; Luo, H.; Pu, E.; Zhang, S.; Dong, H. On the characteristics of Portevin–Le Chatelier bands in cold-rolled 7Mn steel showing transformation-induced plasticity. *Int. J. Plast.* **2018**, *103*, 188–202. [[CrossRef](#)]

90. Shi, J.; Sun, X.; Wang, M.; Hui, W.; Dong, H.; Cao, W. Enhanced work-hardening behavior and mechanical properties in ultrafine-grained steels with large-fractioned metastable austenite. *Scr. Mater.* **2010**, *63*, 815–818. [[CrossRef](#)]
91. Luo, H.; Shi, J.; Wang, C.; Cao, W.; Sun, X.; Dong, H. Experimental and numerical analysis on formation of stable austenite during the intercritical annealing of 5Mn steel. *Acta Mater.* **2011**, *59*, 4002–4014. [[CrossRef](#)]
92. Wang, C.; Shi, J.; Wang, C.; Hui, W.J.; Wang, M.; Dong, H.; Cao, W. Development of ultrafine lamellar ferrite and austenite duplex structure in 0.2C5Mn steel during ART-annealing. *ISIJ Int.* **2011**, *51*, 651–656. [[CrossRef](#)]
93. Wang, X.; Wang, L.; Huang, M. In-situ evaluation of Lüders band associated with martensitic transformation in a medium Mn transformation-induced plasticity steel. *Mater. Sci. Eng. A* **2016**, *674*, 59–63. [[CrossRef](#)]
94. Kucerova, L.; Jirkova, H.; Masek, B. The effect of alloying on mechanical properties of advanced high strength steels. *Arch. Metall. Mater.* **2014**, *59*, 1189–1192. [[CrossRef](#)]
95. Furukawa, T.; Huang, H.; Matsumura, O. Effect of Carbon content on mechanical properties of 5% Mn steels exhibiting transformation induced plasticity. *Mater. Sci. Eng.* **2013**, *10*, 964–970. [[CrossRef](#)]
96. Gramlich, A.; van der Linde, C.; Ackermann, M.; Bleck, W.J.R. Effect of molybdenum, aluminium and boron on the phase transformation in 4 wt.-% manganese steels. *Results Mater.* **2020**, *8*, 100147. [[CrossRef](#)]
97. Garcia-Junceda, A.; Capdevila, C.; Caballero, F.G.; de Andres, C.G. Dependence of martensite start temperature on fine austenite grain size. *Scr. Mater.* **2008**, *58*, 134–137. [[CrossRef](#)]
98. Yang, H.S.; Bhadeshia, H.K.D.H. Austenite grain size and the martensite-start temperature. *Scr. Mater.* **2009**, *60*, 493–495. [[CrossRef](#)]
99. Lee, S.; De Cooman, B.C. On the selection of the optimal intercritical annealing temperature for Medium Mn TRIP steel. *Metall. Mater. Trans. A* **2013**, *44*, 5018–5024. [[CrossRef](#)]
100. Lee, S.J.; Lee, S.; De Cooman, B.C. Martensite transformation of sub-micron retained austenite in ultra-fine grained manganese transformation-induced plasticity steel. *Int. J. Mater. Res.* **2013**, *104*, 423–429. [[CrossRef](#)]
101. Andrews, K.W. Empirical formulae for the calculation of some transformation temperatures. *J. Iron Steel Inst.* **1965**, 721–727.
102. Kamoutsi, H.; Gioti, E.; Haidemenopoulos, G.N.; Cai, Z.; Ding, H. Kinetics of solute partitioning during intercritical annealing of a Medium-Mn steel. *Metall. Mater. Trans. A* **2015**, *46*, 4841–4846. [[CrossRef](#)]
103. Li, X.; Chang, Y.; Wang, C.; Hu, P.; Dong, H. Comparison of the hot-stamped boron-alloyed steel and the warm-stamped medium-Mn steel on microstructure and mechanical properties. *Mater. Sci. Eng. A* **2017**, *679*, 240–248. [[CrossRef](#)]
104. Zhou, Y.; Song, X.; Liang, J.; Shen, Y.; Misra, R. Innovative processing of obtaining nanostructured bainite with high strength-high ductility combination in low-carbon-medium-Mn steel: Process-structure-property relationship. *Mater. Sci. Eng. A* **2018**, *718*, 267–276. [[CrossRef](#)]
105. Morawiec, M.; Grajcar, A.; Zalecki, W.; Garcia-Mateo, C.; Opiela, M. Dilatometric study of phase transformations in 5 Mn steel subjected to different heat treatments. *Materials* **2020**, *13*, 958. [[CrossRef](#)]
106. Liu, C.Y.; Peng, Y.; Kong, L.; Wang, Y.Q. Effect of the deformation degree on the microstructure evolution of an austenite reverted transformation-annealed medium manganese steel. *Metals-Basel* **2020**, *10*, 887. [[CrossRef](#)]
107. Hong, H.; Lee, O.; Song, G. Effect of Mn addition on the microstructural changes and mechanical properties of C-Mn TRIP steels. *J. Korean Soc. Heat Treat.* **2003**, *16*, 205–210.
108. Suh, D.; Park, S.; Lee, T.; Oh, C.; Kim, S. Influence of Al on the microstructural evolution and mechanical behavior of Low-Carbon, Manganese transformation-induced-plasticity steel. *Metall. Mater. Trans. A* **2009**, *41*, 397–408. [[CrossRef](#)]
109. Furukawa, T. Dependence of strength-ductility characteristics on thermal history in low carbon. *Mater. Sci. Eng.* **2013**, *5*, 465–470.
110. Xu, H.; Cao, W.; Dong, H.; Li, J. Effects of Aluminium on the microstructure and mechanical properties in 0.2C–5Mn steels under different heat treatment conditions. *ISIJ Int.* **2015**, *55*, 662–669. [[CrossRef](#)]
111. Zhang, Y.; Shao, C.; Wang, J.; Zhao, X.; Hui, W. Intercritical annealing temperature dependence of hydrogen embrittlement behavior of cold-rolled Al-containing medium-Mn steel. *Int. J. Hydrogen Energy.* **2019**, *44*, 22355–22367. [[CrossRef](#)]
112. Jeong, M.; Park, T.; Choi, S.; Lee, S.; Han, J. Recovering the ductility of medium-Mn steel by restoring the original microstructure. *Scr. Mater.* **2021**, *190*, 16–21. [[CrossRef](#)]
113. Zhang, X.; Hou, H.; Liu, T.; Liu, H.; Zhou, Q.; Zhao, L.; Liu, X.; Cui, H. Properties of a novel heterogeneous cold-rolled medium Mn steel with high product of strength and ductility. *Earth Sci.* **2020**, *33*, 927–934.

114. Oyarzabal, M.; Martinez-De-Guerenu, A.; Gutierrez, I. Effect of stored energy and recovery on the overall recrystallization kinetics of a cold rolled low carbon steel. *Mater. Sci. Eng. A* **2008**, *485*, 200–209. [[CrossRef](#)]
115. Raabe, D.; Sandlobes, S.; Millan, J.; Ponge, D.; Assadi, H.; Herbig, M.; Choi, P.P. Segregation engineering enables nanoscale martensite to austenite phase transformation at grain boundaries: A pathway to ductile martensite. *Acta Mater.* **2013**, *61*, 6132–6152. [[CrossRef](#)]
116. Zhang, X.; Miyamoto, G.; Toji, Y.; Nambu, S.; Koseki, T.; Furuhashi, T. Orientation of austenite reverted from martensite in Fe-2Mn-1.5Si-0.3C alloy. *Acta Mater.* **2018**, *144*, 601–612. [[CrossRef](#)]
117. Klinger, L.; Rabkin, E. Diffusion along the grain boundaries in crystals with dislocations. *Interface Sci.* **1998**, *6*, 197–203. [[CrossRef](#)]
118. Lee, J.; De Cooman, B.C. Development of a press-hardened steel suitable for thin slab direct rolling processing. *Metall. Mater. Trans. A* **2015**, *46a*, 456–466. [[CrossRef](#)]
119. Zhou, J.; Wang, B.; Huang, M.; Cui, D. Effect of hot stamping parameters on the mechanical properties and microstructure of cold-rolled 22MnB5 steel strips. *Int. J. Min. Met. Mater.* **2014**, *21*, 544–555. [[CrossRef](#)]
120. Naderi, M. Hot Stamping of Ultra High Strength Steels. Ph.D. Thesis, RWTH Aachen University, Aachen, Germany, 2008.
121. Production Costs from Energy-Intensive Industries in the EU and Third Countries. 2016. Available online: <https://publications.jrc.ec.europa.eu/repository/bitstream/JRC100101/ldna27729enn.pdf> (accessed on 20 September 2020).
122. Li, S.; Luo, H. A novel high-strength oxidation-resistant press hardening steel sheet requiring no Al-Si coating. In Proceedings of the TMS 2020 149th Annual Meeting and Exhibition, San Diego, CA, USA, 23–27 February 2020; pp. 505–513.
123. Tian, X.W.; Zhang, Y.S.; Li, J. Investigation on tribological behavior of advanced high strength steels: Influence of hot stamping process parameters. *Tribol. Lett.* **2012**, *45*, 489–495. [[CrossRef](#)]
124. Schrenk, M.; Krenn, S.; Ripoll, M.R.; Nevsad, A.; Paar, S.; Grundtner, R.; Rohm, G.; Franek, F. Statistical analysis on the impact of process parameters on tool damage during press hardening. *J. Manuf. Process.* **2016**, *23*, 222–230. [[CrossRef](#)]
125. Garcia Aranda, L.; Chastel, Y.; Fernandez Pascual, J.; Dal Negro, T. Experiments and simulation of hot stamping of quenchable steels. *Adv. Technol. Plast.* **2002**, *2*, 1135–1140.
126. Chang, Y.; Wang, C.Y.; Zhao, K.M.; Dong, H.; Yan, J.W. An introduction to medium-Mn steel: Metallurgy, mechanical properties and warm stamping process. *Mater. Des.* **2016**, *94*, 424–432. [[CrossRef](#)]
127. Hu, B.; Luo, H.W. A strong and ductile 7Mn steel manufactured by warm rolling and exhibiting both transformation and twinning induced plasticity. *J. Alloys Compd.* **2017**, *725*, 684–693. [[CrossRef](#)]
128. Arlazarov, A.; Goune, M.; Bouaziz, O.; Hazotte, A.; Petitgand, G.; Barges, P. Evolution of microstructure and mechanical properties of medium Mn steels during double annealing. *Mater. Sci. Eng. A* **2012**, *542*, 31–39. [[CrossRef](#)]
129. De Cooman, B.C.; Lee, S.J.; Shin, S.; Seo, E.J.; Speer, J.G. Combined intercritical annealing and Q&P processing of Medium Mn steel. *Metall. Mater. Trans. A* **2016**, *48*, 39–45.
130. Dong, H.; Sun, X.; Cao, W.; Liu, Z.; Wang, M.; Weng, Y. On the performance improvement of steels through M-3 structure control. In *Advanced Steels: The Recent Scenario in Steel Science and Technology*; Springer: Berlin, Germany, 2011; pp. 35–57.
131. Xie, Z.; Fang, Y.; Han, G.; Guo, H.; Misra, R.; Shang, C. Structure–property relationship in a 960 MPa grade ultrahigh strength low carbon niobium–vanadium microalloyed steel: The significance of high frequency induction tempering. *Mater. Sci. Eng. A* **2014**, *618*, 112–117. [[CrossRef](#)]
132. Wang, C.; Chang, Y.; Li, X.; Zhao, K.; Dong, H. Relation of martensite-retained austenite and its effect on microstructure and mechanical properties of the quenched and partitioned steels. *Sci. China Technol. Sci.* **2016**, *59*, 832–838. [[CrossRef](#)]
133. Ding, H.; Tang, Z.Y.; Li, W.; Wang, M.; Song, D. Microstructures and mechanical properties of Fe-Mn-(Al, Si) TRIP/TWIP steels. *J. Iron Steel Res. Int.* **2006**, *13*, 66–70. [[CrossRef](#)]
134. Suh, D.W.; Kim, S.J. Medium Mn transformation-induced plasticity steels: Recent progress and challenges. *Scr. Mater.* **2017**, *126*, 63–67. [[CrossRef](#)]
135. Dumay, A.; Chateau, J.P.; Allain, S.; Migot, S.; Bouaziz, O. Influence of addition elements on the stacking-fault energy and mechanical properties of an austenitic Fe–Mn–C steel. *Mater. Sci. Eng. A* **2008**, *483–484*, 184–187. [[CrossRef](#)]

136. Curtze, S.; Kuokkala, V.T.; Oikari, A.; Talonen, J.; Hänninen, H. Thermodynamic modeling of the stacking fault energy of austenitic steels. *Acta Mater.* **2011**, *59*, 1068–1076. [[CrossRef](#)]
137. Lee, C.; Jeong, J.; Han, J.; Lee, S.; Lee, S.; Lee, Y. Coupled strengthening in a medium manganese lightweight steel with an inhomogeneously grained structure of austenite. *Acta Mater.* **2015**, *84*, 1–8. [[CrossRef](#)]
138. Martin, S.; Wolf, S.; Martin, U.; Kruger, L.; Rafaja, D. Deformation mechanisms in austenitic TRIP/TWIP steel as a function of temperature. *Metall. Mater. Trans. A* **2016**, *47a*, 49–58. [[CrossRef](#)]
139. Lee, S.; Lee, K.; De Cooman, B.C. Observation of the TWIP plus TRIP plasticity-enhancement mechanism in Al-added 6 Wt Pct Medium Mn steel. *Metall. Mater. Trans. A* **2015**, *46a*, 2356–2363. [[CrossRef](#)]
140. Suh, D.W.; Ryu, J.H.; Joo, M.S.; Yang, H.S.; Lee, K.; Bhadeshia, H.K.D.H. Medium-alloy Manganese-rich transformation-induced plasticity steels. *Metall. Mater. Trans. A* **2012**, *44*, 286–293. [[CrossRef](#)]
141. Bleck, W.; Guo, X.F.; Ma, Y. The TRIP effect and its application in cold formable sheet steels. *Steel Res. Int.* **2017**, *88*, 1700218. [[CrossRef](#)]
142. Bouaziz, O.; Guelton, N. Modelling of TWIP effect on work-hardening. *Mater. Sci. Eng. A* **2001**, *319*, 246–249. [[CrossRef](#)]
143. Wang, C.; Li, X.; Han, S.; Zhang, L.; Chang, Y.; Cao, W.; Dong, H. Warm stamping technology of the medium Manganese steel. *Steel Res. Int.* **2018**, *89*, 1700360. [[CrossRef](#)]
144. Hou, Z.R.; Opitz, T.; Xiong, X.C.; Zhao, X.M.; Yi, H.L. Bake-partitioning in a press-hardening steel. *Scr. Mater.* **2019**, *162*, 492–496. [[CrossRef](#)]
145. Pan, H.J.; Cai, M.H.; Ding, H.; Huang, H.S.; Zhu, B.; Wang, Y.L.; Zhang, Y.S. Microstructure evolution and enhanced performance of a novel Nb-Mo microalloyed medium Mn alloy fabricated by low-temperature rolling and warm stamping. *Mater. Des.* **2017**, *134*, 352–360. [[CrossRef](#)]
146. Lu, Q.; Eizadjou, M.; Wang, J.; Ceguerra, A.; Ringer, S.; Zhan, H.; Wang, L.; Lai, Q. Medium-Mn martensitic steel ductilized by baking. *Metall. Mater. Trans. A* **2019**, *50*, 4067–4074. [[CrossRef](#)]
147. Heating of Steel: Oxidation and Decarburisation. 2017. Available online: <https://www.engineeringenotes.com/metallurgy/steel/heating-of-steel-oxidation-and-decarburisation-metallurgy/25788> (accessed on 20 September 2020).
148. Hajduga, M.; Kucera, J. Decarburization of Fe-Cr-C steels during high-temperature oxidation. *Oxid. Met.* **1988**, *29*, 419–433. [[CrossRef](#)]
149. Silveira, C.C.; da Cunha, M.A.; Buono, V.T.L. The influence of internal oxidation during decarburization of a grain oriented silicon steel on the morphology of the glass film formed at high temperature annealing. *J. Magn. Magn. Mater.* **2014**, *358*, 65–69. [[CrossRef](#)]
150. Zheng, G.; Li, X.; Chang, Y.; Wang, C.; Dong, H. A comparative study on formability of the third-generation automotive Medium-Mn steel and 22MnB5 steel. *J. Mater. Eng. Perform.* **2018**, *27*, 530–540. [[CrossRef](#)]

Publisher’s Note: MDPI stays neutral with regard to jurisdictional claims in published maps and institutional affiliations.



© 2020 by the authors. Licensee MDPI, Basel, Switzerland. This article is an open access article distributed under the terms and conditions of the Creative Commons Attribution (CC BY) license (<http://creativecommons.org/licenses/by/4.0/>).